

Comparative Study of Land Surface  
Models Coupled to WRF Used in  
the Sensitive Analysis Performed  
in the NEWA Project

A. M.<sup>a</sup> Palomares Losada  
E. García Bustamante  
J. Navarro Montesinos  
F. González Rouco



## Comparative Study of Land Surface Models Coupled to WRF Used in the Sensitive Analysis Performed in the NEWA Project

A.M.<sup>a</sup> Palomares Losada<sup>(1)</sup>

E. García Bustamante <sup>(1)</sup>

J. Navarro Montesinos <sup>(1)</sup>

F. González Rouco <sup>(2)</sup>

(1) CIEMAT

(2) UNIVERSIDAD COMPLUTENSE DE MADRID

Publication available in [General catalog of official publications](#)

© CIEMAT, 2019

Legal Deposit: xxxx

ISSN: xxxx

NIPO: xxxx

**Edition and Publication:**

Editorial CIEMAT

Avda. Complutense, 40 28040-MADRID

e-mail: [editorial@ciemat.es](mailto:editorial@ciemat.es)

[Editorial news](#)

CIEMAT do not share necessarily the opinions expressed in this published work, whose responsibility corresponds to its author(s).

All rights reserved. No part of this published work may be reproduced, stored in a retrieval system, or transmitted in any form or by any existing or future means, electronic, mechanical, photocopying, recording, or otherwise, without written permission from the publisher.

## COMPARATIVE STUDY OF LAND SURFACE MODELS COUPLED TO WRF USED IN THE SENSITIVE ANALYSIS PERFORMED IN THE NEWA PROJECT

Palomares Losada, A.M.<sup>a</sup>; García Bustamante, E.; Navarro Montesinos, J.; González Rouco, F.

69 pp., 24 fig., 5 tables, 79 ref.

### Abstract:

All the processes addressed in Land Surface Models (LSMs) are relevant for the simulation of the atmosphere, since the LSM provide the surface layer initial and boundary conditions. This document is a synthesis of bibliographic research on LSMs that can optionally be used in the WRF regional model: 5-Layer Thermal diffusion, Noah, Noah-MP, RUC, Pleim and Xiu, SSiB and CLM. The treatment for the main biogeophysical feedbacks between the land surface and the atmosphere are analyzed for each one of the models and compared to one another in order to facilitate the interpretation of the WRF model performance in experiments with different LSM configurations to simulate the surface wind field. There is not a single criterion to ascertain which one of the LSMs performs best but it can be concluded that both Noah-MP and CLM are the most complex models and allow for more realistic vertical energy diffusion with influences for hydrology and the surface energy balance.

## ESTUDIO COMPARATIVO DE MODELOS DE SUELO ACOPLADOS A WRF PARA EL ANÁLISIS DE SENSIBILIDAD REALIZADO EN EL PROYECTO NEWA

Palomares Losada, A.M.<sup>a</sup>; García Bustamante, E.; Navarro Montesinos, J.; González Rouco, F.

69 pp., 24 fig., 5 tables, 79 ref.

### Resumen:

Todos los procesos abordados en los Modelos de suelo (LSMs) son relevantes para la simulación de la atmósfera, ya que el LSM proporciona las condiciones iniciales y de contorno en la superficie terrestre. Este documento es una síntesis de la investigación bibliográfica sobre los LSMs que pueden ser utilizados opcionalmente en el modelo regional WRF: modelo de 5 capas, Noah, Noah-MP, RUC, Pleim y Xiu, SSiB y CLM. El tratamiento para las principales retroalimentaciones biogeofísicas entre la superficie terrestre y la atmósfera se analiza para cada uno de los modelos y se compara entre sí para facilitar la interpretación del comportamiento del modelo WRF en experimentos con diferentes configuraciones de LSM, para simular el viento en superficie. No existe un criterio único para determinar cuál de los LSM funciona mejor, aunque se puede concluir que tanto Noah-MP como CLM son los modelos más complejos y con mayor realismo en la difusión vertical de energía, con efectos sobre la hidrología y el equilibrio energético de la superficie.

# TABLE OF CONTENTS

<b>1</b>	<b>INTRODUCTION.....</b>	<b>1</b>
<b>2</b>	<b>ROLE PLAYED BY THE LAND SURFACE IN ATMOSPHERIC PROCESSES.....</b>	<b>3</b>
2.1	THE SURFACE ENERGY BALANCE .....	3
2.2	THE SURFACE WATER BALANCE .....	7
2.3	THE CLIMATIC EFFECT OF SNOW .....	8
2.4	CARBON .....	9
<b>3</b>	<b>EVOLUTION OF LAND SURFACE MODELS.....</b>	<b>11</b>
3.1	FIRST-GENERATION MODELS.....	11
3.2	SECOND-GENERATION MODELS.....	12
3.3	THIRD-GENERATION MODELS .....	13
<b>4</b>	<b>LSMS COUPLED TO WRF .....</b>	<b>16</b>
<b>5</b>	<b>FIVE -LAYER THERMAL DIFFUSION MODEL .....</b>	<b>18</b>
<b>6</b>	<b>NOAH MODEL.....</b>	<b>19</b>
6.1	ORIGIN AND EVOLUTION .....	19
6.2	MODEL CHARACTERISTICS .....	20
<b>7</b>	<b>NOAH-MP MODEL .....</b>	<b>24</b>
7.1	ISSUES IN THE NOAH LSM.....	24
7.2	TRANSITION FROM THE NOAH LSM TO THE NOAH-MP LSM .....	24
7.3	MAIN AUGMENTATIONS TO THE NOAH LSM.....	25
<b>8</b>	<b>RAPID UPDATE CYCLE MODEL (RUC) .....</b>	<b>28</b>
8.1	MODEL OVERVIEW.....	28
8.2	MODEL PHYSICS.....	28
8.3	OPERATIONAL ASPECTS OF THE RUC LSM .....	30
8.4	MODIFICATIONS IN THE WRF VERSION .....	30
<b>9</b>	<b>PLEIM AND XIU MODEL (PX) .....</b>	<b>33</b>

9.1	MODEL OVERVIEW.....	33
9.2	SOIL MOISTURE AND THERMODINAMICS .....	33
9.3	SOIL PARAMETERS.....	33
9.4	VEGETATION PARAMETERS AND TYPES.....	34
9.5	SNOW TREATMENT .....	34
9.6	DATA ASSIMILATION .....	35
10	SIMPLIFIED BIOSPHERE MODEL (SIB) .....	36
10.1	MODEL OVERVIEW.....	36
10.2	MODEL STRUCTURE.....	36
10.3	IMPROVEMENTS IN THE SIB MODEL .....	39
11	COMMUNITY LAND MODEL (CLM).....	41
11.1	MODEL HISTORY AND OVERVIEW .....	41
11.2	MAIN CHARACTERISTICS OF THE CLM4 LSM .....	43
11.3	MODEL REQUIREMENTS .....	48
12	LAND SURFACE MODELS COMPARISON .....	50
12.1	SOIL LAYERS.....	50
12.2	LAND USE AND SOIL TEXTURE.....	51
12.3	CANOPY STRUCTURE, VEGETATION SCHEME AND DATA ASSIMILATION .....	52
12.4	HYDROLOGY.....	54
12.5	SNOW LAYERS.....	56
13	CONCLUSIONS.....	59
14	REFERENCES.....	62

## TABLE OF FIGURES

Figure 1	Schematic diagram of the annual mean global energy balance. Units are percentage of incoming solar radiation. The solar (shortwave) fluxes are shown on the left-hand side and the terrestrial (longwave) fluxes are on the right-hand side (redrawn from Rosen, 1999) .....	4
Figure 2	Diagram of the impact an increase in albedo has on the land surface and some elements of the boundary-layer climate (redrawn from Pitman, 2003) .....	5
Figure 3	Diagram of the impact decrease in root depth has on the land surface and some elements of the boundary-layer climate (redrawn from Pitman, 2003) .....	5
Figure 4	Diagram of the impact that decrease in the leaf area index (LAI) has on the land surface and some elements of the boundary-layer climate (redrawn from Pitman, 2003) .....	6
Figure 5	Diagram of the impact decrease in the roughness length has on the land surface and some elements of the boundary-layer climate (redrawn from Pitman, 2003) .....	7
Figure 6	Diagram of the impact of decrease in soil moisture on the land surface and some elements of the boundary-layer climate (redrawn from Pitman,2003) .....	8
Figure 7	Diagram of the impact of increased CO <sub>2</sub> on the land surface and some elements of the boundary-layer climate surface and some elements of the boundary-layer climate (redrawn from Pitman, 2003).....	9
Figure .8.	Land biogeophysical and hydrologic processes simulated by a LSM (Oleson et al.,2010).....	10
Figure 9	Illustration of a first-generation land surface model. Terms not defined in the text are the reference height for temperature $T_r$ , the maximum soil moisture capacity ( $W_{max}$ ) and the soil moisture content $w$ . Modified from (Sellers et al.,1997).....	11
Figure 10	Illustration of a second-generation land surface model. Terms not defined in the text are the reference height for temperature $T_r$ , the maximum soil moisture capacity ( $W_{max}$ ) and the soil moisture content $w$ . Modified from (Sellers et al.,1997).....	13
Figure 11	Illustration of a third –generation land surface model. Terms not defined in the text are the reference height for temperature, $T_r$ , the maximum soil moisture capacity ( $W_{max}$ ) and the soil moisture content $w$ . Modified from (Sellers et al., 1997).....	14
Figure 12	Schematic of the increasing levels of detail being added into surface modeling approaches .....	15

Figure 13	Timeline of the Noah Landsurface Model evolution with references to relevant Model Physics and /or Land Surface fields implemented in the NCEP operational Mesoscale Eta Model (Ek et al., 2003) .....	19
Figure 14	Schematic representation of the Noah LSM.....	21
Figure 15	Schematic representation of the Noah-MP LSM .....	25
Figure 16	Schematic representation of the RUC LSM .....	29
Figure 17	Modifications to the RUC LSM implemented in the WRF version 3.6 model (2014) compared to its predecessor 2000 version. Abbreviations: MODIS 5 Moderate Resolution Imaging Spectroradiometer; FPAR 5 fractional photosynthetically active radiation; IGBP 5 International Geosphere-Biosphere Programme; AVHRR 5 Advanced Very High Resolution Radiometer; LAI 5 leaf area index; DMSP 5 Defense Meteorological Satellite Program .....	31
Figure 18	Vegetation morphology as represented in the Simple Biosphere Model (SiB) ..	37
Figure 19	Root systems and soil layer of the Simple Biosphere Model (SiB) .....	38
Figure 20	Framework of the Simple Biosphere Model (SiB).....	38
Figure 21	Framework of the modified Simple Biosphere Model (SiB3) .....	40
Figure 22	Current default configuration of the CLM subgrid hierarchy emphasizing the vegetated landunit. Only four PFTs are shown associated with the single column beneath the vegetated landunit but up to sixteen are possible.....	43
Figure 23	Typical one dimensional Soil Column in LSM Coupled with Multiple Land Surface Hydrologic Processes .....	44
Figure 24	Biogeophysical processes in CLM4 (from Lawrence et al, 2010) .....	47

## TABLE OF TABLES

Table 1	Soil layers characteristics in the 5-Layer, Noah, Noah-MP, RUC, Pleim and Xiu (PX), SSiB and CLM and models .....	51
Table 2	Land-use and soil texture categories in the 5-Layer, Noah, Noah-MP, RUC, Pleim and Xiu (PX), SSiB and CLM and models .....	52
Table 3	Canopy structure, vegetation scheme and data assimilation in the 5-Layer, Noah, Noah-MP, RUC, Pleim and Xiu (PX), SSiB and CLM and models .....	53
Table 4	Hydrology, soil moisture, groundwater interaction and related runoff production in the 5-Layer, Noah, Noah-MP, RUC, Pleim and Xiu (PX), SSiB and CLM and models .....	55
Table 5	Snow treatment in the 5-Layer, Noah, Noah-MP, RUC, Pleim and Xiu (PX), SSiB and CLM and models .....	57



# 1 INTRODUCTION

During the 80s many sensitivity experiments were performed with General Circulation Models (CGMs) involving changing the surface characteristics such as albedo, humidity, moisture availability or roughness that showed a great interdependence between the climatic behavior of the atmosphere and the land surface processes (e.g. Rowntree,1983, etc). At smaller scales, several experiments performed with 2D and 3D models also showed the influence of the soil nature and of its vegetation coverage on the atmospheric circulation (Benjamin,1986, etc.), leading to the conclusion that, it was necessary to improve the representation of land surface processes in both large-scale and mesoscale atmospheric models (Noilhan and Planton,1989).

There is evidence that the land surface is a key component of climate models. It controls the partitioning of available net radiation into sensible and latent heat fluxes. Particularly, the evolution and maximum depth of the Planetary Boundary Layer (PBL) is highly dependent on this partitioning. In addition, mesoscale fluxes of heat due to secondary circulations, caused by spatially varying land use, have been shown to be of the same order of magnitude as turbulent fluxes.

The land surface also controls the partitioning of available water between evaporation and runoff. Besides, the land surface is also the location of the terrestrial carbon sink. Evidence is increasing that the influence of the land surface is significant on climate, and that changes in the land surface can influence regional to global scale climate, on time scales from days to millennia. Furthermore, there is a suggestion that the terrestrial carbon sink may decrease as global temperatures increase as a consequence of rising  $CO_2$  levels (Pitman, 2003).

On the one hand, land-cover and land-use change can alter surface properties in ways that can significantly affect climate, especially at the regional scale and at the surface. The replacement of natural grasslands and forest cover with crops can cause surface cooling (Subin et al., 2011). Global historical land-cover change may have weakened Northern Hemisphere Hadley circulation while causing regional temperature changes of up to 5 degrees (Feddema et al., 2005a) whereas future expansion of agricultural land may continue to warm the tropics while cooling mid latitudes (Feddema et al., 2005b); conversely, intentional afforestation in low latitudes could cause local cooling (Narisma and Pitman, 2006). If a land-cover change occurs over a large enough region, changes in cloudiness and regional circulation may occur that cause subsequent changes in regional climate, including altered regional precipitation.

On the other hand, intentional afforestation for mitigating greenhouse gas emissions via carbon sequestrations is another form of land-cover change that could affect regional climate, since adding trees causes two primary contrasting effects: decreases in surface shortwave albedo, which tend to increase surface air temperature, and increases in evapotranspiration, which tend to reduce surface air temperature (Subin et al., 2011). Temperature changes are dominated by the albedo, which decreases in boreal zones, whereas the evapotranspiration

increases in the tropics and the two effects are often comparable in temperate zones. For temperate zones, several climate model studies have found that the albedo effect predominates and causes surface warming, especially when forest is being replaced. Besides, the amount and duration of snow cover, which have a strong influence on the magnitude and timing of the albedo effect, vary widely in temperate areas.

All the examples mentioned above show the importance of the land surface-atmosphere interaction for climate considerations, but it is also crucial for the atmosphere in the numerical weather prediction mesoscale models. Due to their role of providing the surface boundary conditions to the atmosphere, the land surface processes are critical in influencing the PBL structure, associated clouds and precipitation processes. As mesoscale models continue to increase in spatial resolution, the density of the observation network is unable to capture the initial mesoscale structure at small scales. The majority of such mesoscale structures that are missed by the observation network are, in reality, a result of land surface forcing by topography, soil moisture, surface vegetation, and soil characteristics. Therefore, it is paramount that mesoscale models include an advanced and robust Land Surface Model (LSM) in order to properly initialize the state of the ground during a data assimilation period and to subsequently capture the mesoscale structures in the free atmosphere and PBL forced by the ground surface (Chen and Dudhia, 2001).

The main task of a Land Surface Model (LSM) in a numerical weather prediction (NWP) model is to accurately partition the available net radiation into soil, latent and sensible heat flux. The last two govern the exchange of heat between the land and the atmosphere, and influence the structure of the Planetary Boundary Layer (PBL).

This document is the result of analysing bibliography on Land Surface models that can optionally be used in the Weather Research, and Forecasting model WRF (Skamarock et al., 2008). The text is focused on understanding the characteristics of the different LSMs, in order to facilitate the interpretation of the WRF model behaviour in experiments in which different configurations can be used to simulate the surface wind field. It has been developed in the context of the NEWA project ([New European Wind Atlas](#))

The most important factors, regarding the inter-influence between the land surface and the atmosphere, that need to be taken into account in the atmosphere processes, and therefore, in the atmospheric models, will be analyzed in Section 2. The evolution of Land Surface Models from the early simple models to the third generation ones will be reviewed in Section 3. The most important characteristics of seven land-surface options included in the WRF model will be analyzed in Sections 5 to 11, and compared to each other in Section 12, in order to search for the differences that could give rise to the corresponding differences in simulations with different WRF LSM configurations.

## 2 ROLE PLAYED BY THE LAND SURFACE IN ATMOSPHERIC PROCESSES

The definition of the 'land surface' used here is the surface that comprises vegetation, soil and snow, including their interactions regarding the exchange of water, energy and carbon within the Earth system. The evidence is now very strong that regional-scale land surface perturbations cause continental-scale changes in climate. There is also evidence that regional-scale land surface changes in key regions can cause significant changes in geographically remote areas via atmospheric teleconnections. Therefore, climate models appear to be sensitive to the land surface because these changes affect the exchange of water, energy, momentum and carbon. In this section a theoretical examination of why the land surface should matter in climate and atmospheric models is presented.

The key processes that need to be represented in the LSM and influence directly the atmosphere are: short and long wave radiation (radiative fluxes), momentum, sensible and latent heat fluxes. Of course, there are many other important processes through which the land surface influences the atmosphere like down-surface heat, moisture transfer and distribution, root absorption of water, direct evaporation and evapotranspiration, subsurface drainage and superficial runoff, the effect of soil and snow temperatures, stomatal resistance and photosynthesis that have been progressively included in the land surface models (Oleson et al., 2010).

Therefore, the fundamental equations that represent the key role played by the surface in the atmospheric dynamics are the two equations that represent the surface energy balance and the surface water balance. There are also many other processes that should be taken into account like the momentum exchange, the climatic effect of snow and the carbon balance, among others.

### 2.1 THE SURFACE ENERGY BALANCE

Although the average values of the different contributions to the surface energy balance are well known (Figure 1, Rosen, 1999), it is important to review both the figures and the concepts themselves, of the most important factors that should be taken into account in this balance.

The shortwave radiation emitted by the Sun is reflected, absorbed or transmitted by the atmosphere. An amount of solar short wave radiation  $S_{\downarrow}$  reaches the Earth's surface and some is reflected (depending on the albedo  $\alpha$ ). Of 100 units of energy entering the global climate system, 46 are absorbed by the surface. Long wave radiation is also received ( $L_{\downarrow}$ ) and emitted ( $L_{\uparrow}$ ) by the Earth surface (depending on the temperature and emissivity of the land and atmosphere). The net balance of the incoming and reflected shortwave radiation and the incoming and emitted longwave radiation at the Earth's surface is called net radiation  $R_n$ :

$$R_n = S_{\downarrow} (1 - \alpha) + L_{\downarrow} - L_{\uparrow}$$

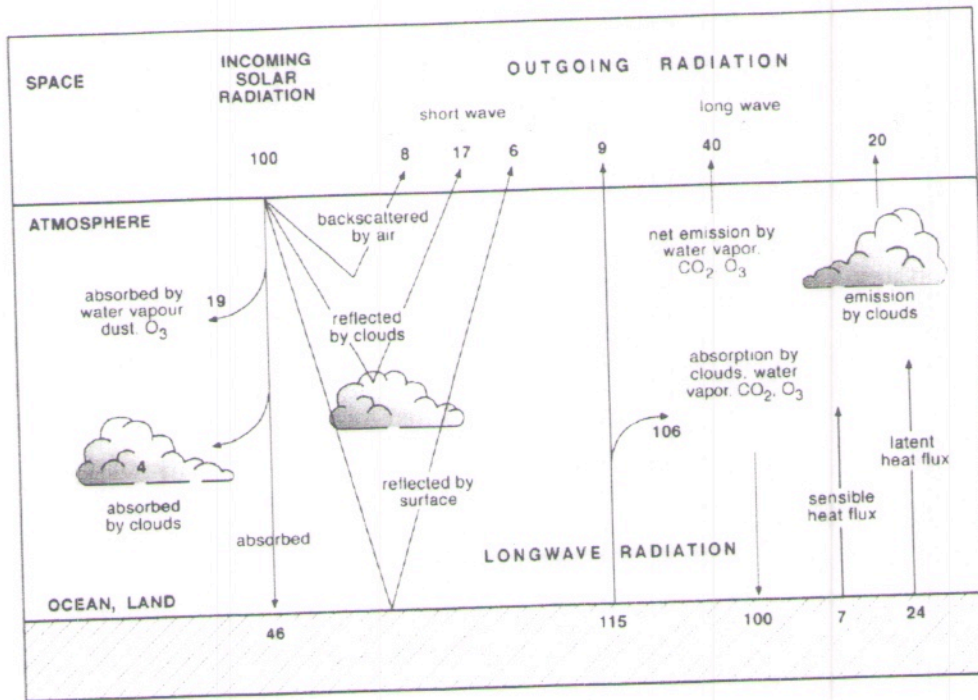


Figure 1 Schematic diagram of the annual mean global energy balance. Units are percentage of incoming solar radiation. The solar (shortwave) fluxes are shown on the left-hand side and the terrestrial (longwave) fluxes are on the right-hand side (redrawn from Rosen, 1999)

Of the 100 units of energy entering the global climate system, 31 are exchanged as sensible and latent heat fluxes, otherwise known as the turbulent energy fluxes. The land surface significantly influences the way that these 31 units of energy are partitioned between sensible H and latent heat  $\lambda E$  fluxes, and also acts as a significant medium to store energy on diurnal, seasonal and longer time scales (thousands of years in the case of heat stored in permafrost).  $R_n$  must be balanced by H,  $\lambda E$ , the soil heat flux G and the chemical energy F stored during photosynthesis and released by respiration (which is usually omitted in climate models as it amounts to less than 1% of absorbed insolation; Sellers, 1992):

$$R_n = H + \lambda E + G + F$$

Changes in the surface albedo affect  $R_n$ , and thus H and  $\lambda E$ . Albedo changes naturally with solar insolation angle, seasonally with vegetation changes and stochastically with  $CO_2$ . In terms of atmospheric modelling, it is important to partition  $R_n$  between H and  $\lambda E$  as well as possible, since less  $\lambda E$  contributes less water vapour to the atmosphere and tends towards decreasing cloudiness and precipitation, whereas decreases in H tend to cool the planetary boundary layer and reduce convection. Complex feedbacks exist whereby changes in clouds or precipitation feedback to modify the initial perturbation to albedo (Figure 2, Pitman, 2003). In this figure, as well as in the following figures in this section, the dotted lines represent a positive feedback and the dashed lines represent a negative feedback.

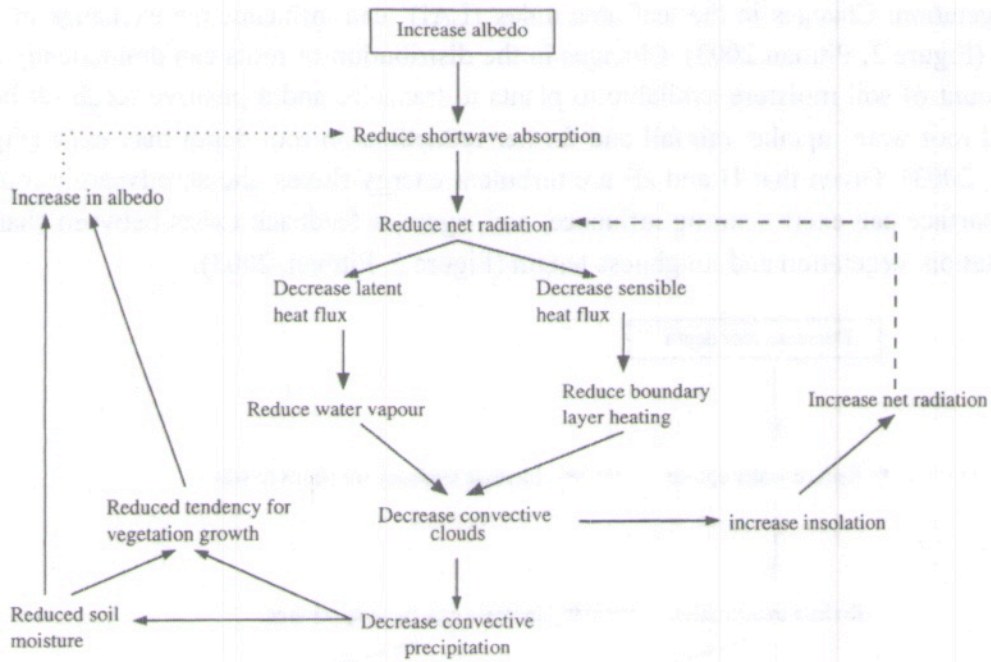


Figure 2 Diagram of the impact an increase in albedo has on the land surface and some elements of the boundary-layer climate (redrawn from Pitman, 2003)

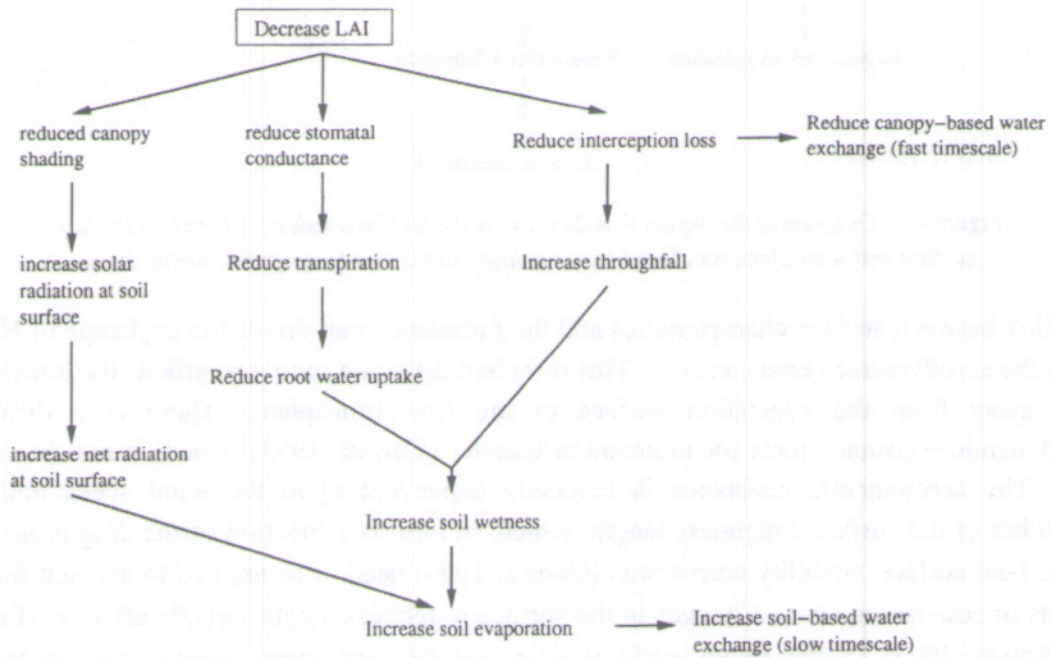


Figure 3 Diagram of the impact decrease in root depth has on the land surface and some elements of the boundary-layer climate (redrawn from Pitman, 2003)

It is also necessary to simulate the diurnal, seasonal and longer term variations in  $H$  and  $\lambda E$  these fluxes as well as possible, for the land surface processes to be represented in atmospheric models (Pitman, 2003).  $H$  and  $\lambda E$  are sensitive to the nature of the land surface in many ways (Verstraete and Dickinson, 1986). Changes in the vegetation cover alter the surface area of vegetation in contact with the atmosphere and the balance between fluxes from the soil

and vegetation. Changes in the leaf area index (LAI)<sup>1</sup> can influence the exchange of both H and  $\lambda E$  (Figure 3, Pitman 2003). Changes in the distribution of roots can dramatically change the amount of soil moisture available to plants to transpire and a positive feedback between reduced root water uptake, rainfall and further reductions in root depth may exist (Figure 4, Pitman, 2003). Given that H and  $\lambda E$  are turbulent energy fluxes, the aerodynamic roughness of the surface can exert a strong influence, and, again, a feedback exists between changes in precipitation, vegetation and roughness length (Figure 5, Pitman, 2003).

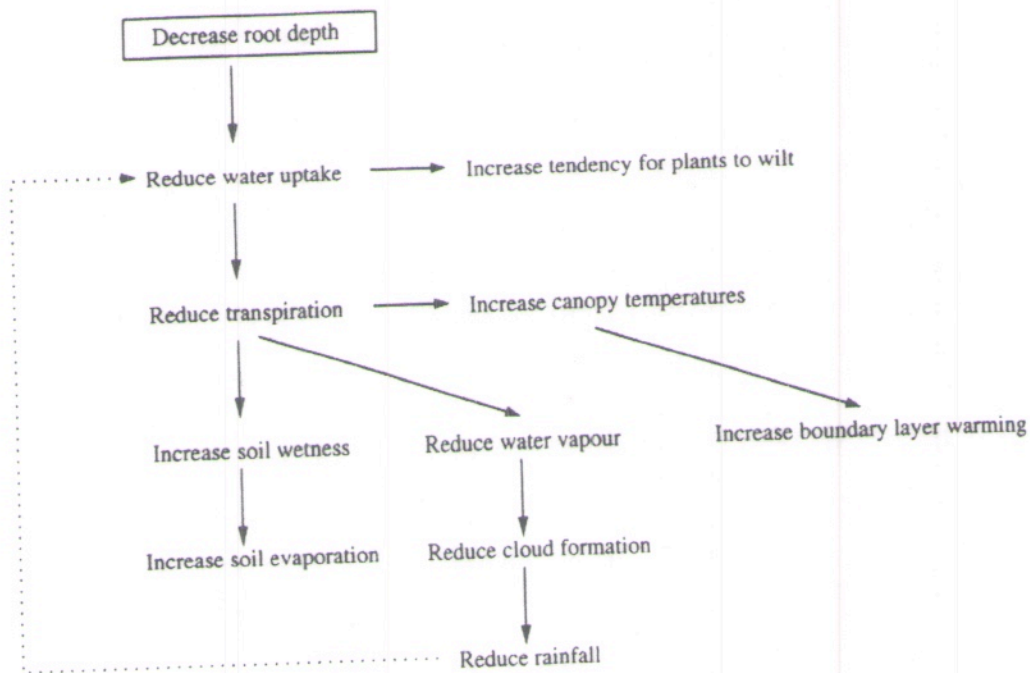


Figure 4 Diagram of the impact that decrease in the leaf area index (LAI) has on the land surface and some elements of the boundary-layer climate (redrawn from Pitman, 2003)

The link between surface characteristics and the turbulence that drives the exchange of H and  $\lambda E$  is the aerodynamic resistance,  $r_a$ <sup>2</sup>. This turbulent diffusion term also affects the transfer of  $CO_2$  away from the vegetation surface to the free atmosphere. There is a different aerodynamic resistance term for momentum transfer (Garratt, 1993), which is not discussed here. The aerodynamic resistance is inversely dependent upon the wind speed and the logarithm of the surface roughness length, which, in turn, is a function of the drag properties of the land surface. Stability corrections (Garratt, 1993) need to be applied to account for the effects of convection on  $r_a$ . Changes in the surface roughness length directly affect  $r_a$  (Figure 5, Pitman, 2003). Since rough surfaces (e.g. forests) are more tightly coupled to the atmosphere than a smooth surface (e.g. grass), a higher roughness length permits a greater

<sup>1</sup> LAI: dimensionless quantity that characterizes plant canopies, defined as the one-sided green leaf area per unit ground surface area in broadleaf canopies

<sup>2</sup>  $r_a$ . Also called drag or aerodynamic drag, is the component of force exerted by the air on a liquid or solid object (such as a raindrop or airplane) that is parallel and opposite to the direction of flow relative to the object.

exchange of  $H$  and  $\lambda E$  for a given set of meteorological conditions. The changes in the surface roughness, will directly affect the exchange of  $H$ ,  $\lambda E$ ,  $CO_2$  and momentum.

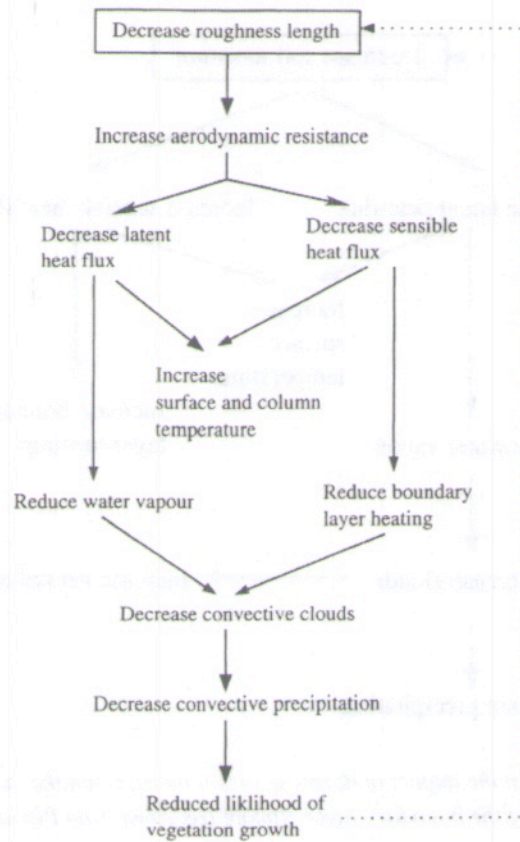


Figure 5 Diagram of the impact decrease in the roughness length has on the land surface and some elements of the boundary-layer climate (redrawn from Pitman, 2003)

Thus, the key characteristics of the land surface, in terms of influencing the exchange of  $H$ ,  $\lambda E$  and  $CO_2$  with the atmosphere, are the albedo, roughness length and the characteristics of plants that influence their surface area (LAI) or their ability to take up water from the soil (roots) and transpire it (LAI, and the resistance exerted by stomates on transpiration and  $CO_2$  uptake). A major impact of changes in the nature of the land surface is the effect on the time scale of surface-atmospheric exchanges. Extremes, especially temperature, are affected by the nature of the surface and whether moisture can be supplied for evaporation and cooling. Thus, modifications in the nature of the land surface could be expected to affect not only mean surface-atmospheric exchanges, but also the extremes and the time scale of the response of the land surface to various external perturbations.

## 2.2 THE SURFACE WATER BALANCE

Precipitation that falls to the Earth's surface is either intercepted by vegetation or reaches the soil surface directly. Precipitation that is intercepted either evaporates or drips to the surface, and the drip, combined with the rainfall that reaches the surface directly, either infiltrates or runs across the soil surface. This constitutes the surface runoff, which usually split between a

fast component ( $R_{surf}$ ) and a slow component ( $R_{drain}$ ). Water that infiltrates may evaporate from the soil surface, drain through the soil, or be taken up by roots and transpired, (Pitman, 2003).

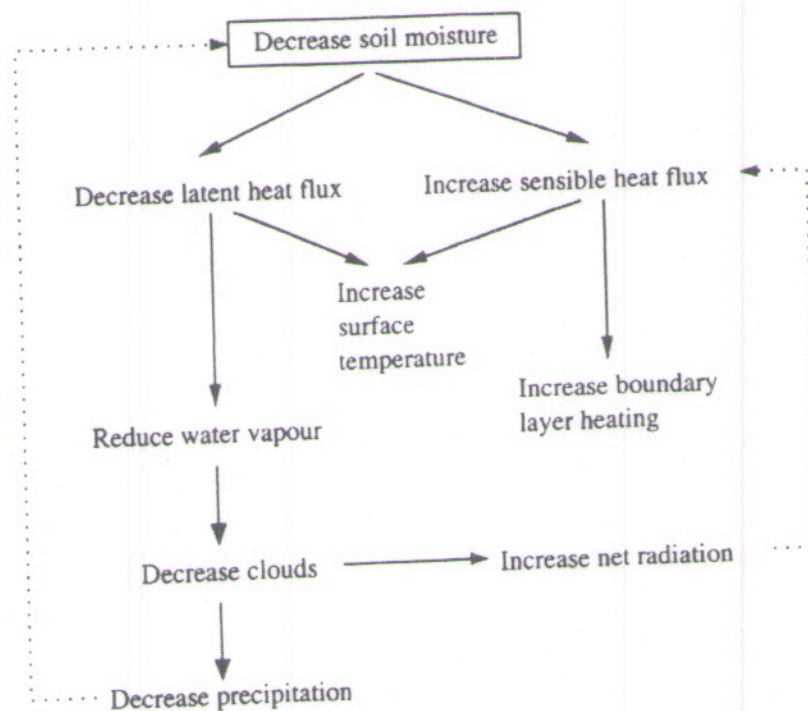


Figure 6 Diagram of the impact of decrease in soil moisture on the land surface and some elements of the boundary-layer climate (redrawn from Pitman, 2003)

A land surface should be able to correctly partition available water (assumed here to be precipitation,  $P$ , but it could also include snow melt) between evaporation  $E$  and runoff. The balancing of incoming and outgoing fluxes of water is called the surface water balance:

$$P = E - R_{drain} - R_{surf} - \Delta S$$

where  $\Delta S$  is the change in soil moisture storage.

A change in vegetation nature affects interception and transpiration (Figure 2-5). A change in the distribution of vegetation modifies the balance between fluxes originated from the soil and those derived through Canopy processes. Changes in evapotranspiration, soil evaporation, re-evaporation of intercepted water, etc. affect runoff and soil moisture content. These then affect a variety of other processes through the link with the surface energy balance (Figure 6, Pitman, 2003).

### 2.3 THE CLIMATIC EFFECT OF SNOW

The properties of snow (e.g. high albedo, low roughness length and low thermal conductivity) lead to impacts at the global scale showed that, over the Eurasian continent, between 18 and 52% of variance in winter temperature could be explained by the extent of snow cover present



in autumn, and that extensive snow cover over continental areas leads to the development of anticyclonic conditions (Barnett et al.,1989). In effect, snow has a substantial impact on climate (Cohen and Rind,1991). Snow is also one of the key feedbacks within the climate system and plays a very strong role as a positive feedback, enhancing the initial impacts of perturbations on the land surface. The representation of snow in climate models has, therefore, been seen as a priority since the first climate models were constructed.

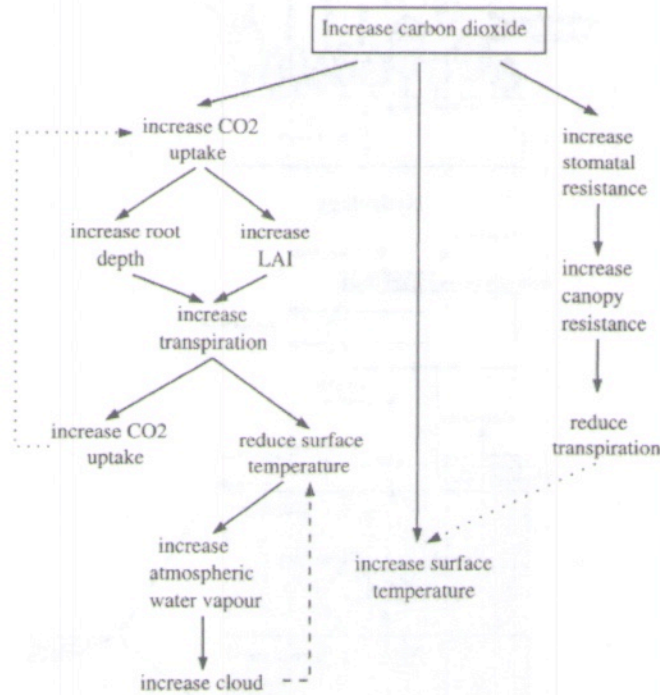


Figure 7 Diagram of the impact of increased CO<sub>2</sub> on the land surface and some elements of the boundary-layer climate surface and some elements of the boundary-layer climate (redrawn from Pitman, 2003)

## 2.4 CARBON

A major purpose of climate models is to simulate the evolution of climate over the next two centuries. Given that CO<sub>2</sub> concentrations will increase over that time period, and that the increase is a major forcing mechanism on climate (Figure7, Pitman, 2003), the ability to represent the impact of land surface processes on atmospheric CO<sub>2</sub> concentrations, and possible long-term net sources or sinks resulting from changes in the biosphere, are priorities in LSMs.

There are good theoretical reasons why the land surface should affect the climate and the simulations by climate models via changes in H, λE, temperature, runoff, carbon and momentum transfer. The Figure 8 shows the overall land biogeophysical and hydrologic processes that need to be accounted for in a land surface model (Oleson et al., 2010).

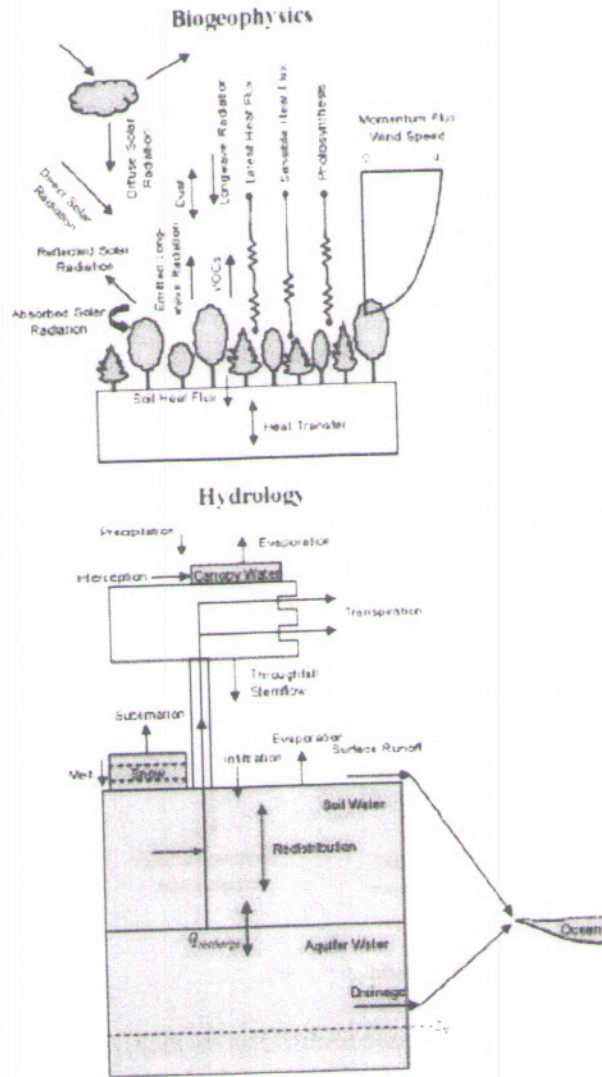


Figure .8. Land biogeophysical and hydrologic processes simulated by a LSM (Oleson et al.,2010)

### 3 EVOLUTION OF LAND SURFACE MODELS

An LSM should represent those processes that take place on the land surface and influence the atmosphere at different time scales. The LSMs have evolved from the first simple ones to the most sophisticated current models. In this section, the evolution of LSM since the first to the third-generation models is presented.

#### 3.1 FIRST-GENERATION MODELS

The first LSM was implemented by (Manabe,1969) into a climate model that intentionally included a simple and idealized distribution of the oceans and continents and did not attempt to represent the seasonal or diurnal cycle. This LSM used a simple energy balance equation, ignoring heat conduction into the soil (a reasonable assumption given the lack of the diurnal or seasonal cycle). (Manabe,1969) implemented a globally constant soil depth and water-holding capacity, where evaporation was limited by soil water content below a threshold; if the soil moisture exceeded a prescribed limit, then further precipitation generated runoff. This parameterization of hydrology is commonly called the 'Manabe bucket model'. An illustration of the basic conceptual design of this first-generation model is shown in (Figure 9).

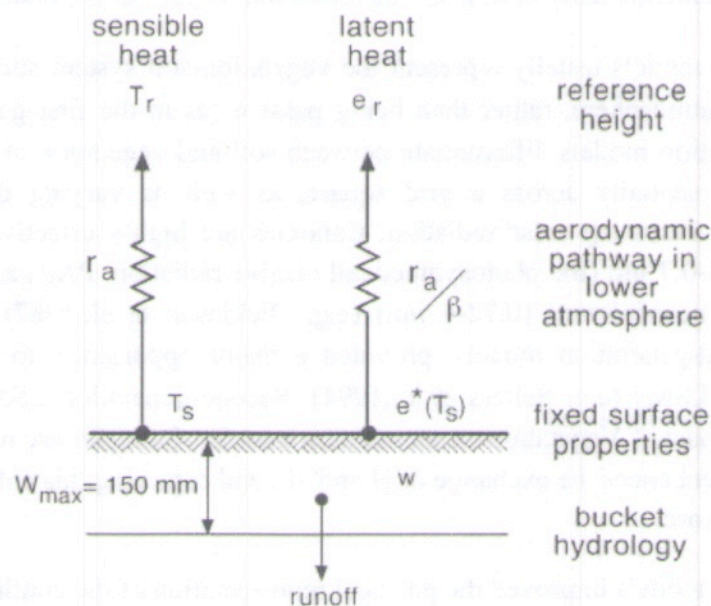


Figure 9 Illustration of a first-generation land surface model. Terms not defined in the text are the reference height for temperature  $T_r$ , the maximum soil moisture capacity ( $W_{max}$ ) and the soil moisture content  $w$ . Modified from (Sellers et al.,1997)

The (Manabe,1969) LSM and a generation of simpler schemes were described by (Sellers et al.,1997) as first-generation models. This is a useful generalization, although (Sellers et al.,1997) based their classification largely on the level of complexity of the evapotranspiration processes. Their classification recognized that there was a group of LSMs that used simple

bulk aerodynamic transfer formulations and tended to use uniform and prescribed surface parameters, including water-holding capacity, albedo and roughness length. Vegetation and the role of vegetation (Verstraete and Dickinson, 1986) was treated implicitly and did not change in time.

### 3.2 SECOND-GENERATION MODELS

A fundamental step forward in land surface modelling took place in 1978 when (Deardorff, 1978) introduced a method for simulating soil temperature and moisture in two layers and vegetation as a single bulk layer (Figure 10). Deardorff represented a revolution in land surface modelling, since processes were treated explicitly and mathematically and this provided an opportunity for a generation of micrometeorologists to contribute to LSM development.

The two key players were R. E. Dickinson and P. J. Sellers, who developed LSMs that built philosophically on (Deardorff, 1978). The two LSMs, the Biosphere Atmosphere Transfer Scheme (BATS) (Dickinson et al., 1986), and the Simple Biosphere Model (SiB) (Sellers et al., 1986), continue to be developed and form the basis for some major new innovations, such as the Common Land Model (Dai et al., 2003). There are a very large number of second-generation models that are innovative in the way some components have been developed or tested, but all are fundamentally built from the leadership of Deardorff, Dickinson and Sellers.

Second-generation models usually represent the vegetation-soil system such that the surface interacts with the atmosphere, rather than being passive (as in the first-generation models). The second-generation models differentiate between soil and vegetation at the surface; thus, albedo may vary spatially across a grid square, as well as varying depending on the wavelength of the incoming solar radiation. Canopies are highly effective at absorbing in wavelengths of 0.4-0.7  $\mu\text{m}$  (the photosynthetically active radiation, PAR) and are moderately reflective in the near-infrared (0.72-4  $\mu\text{m}$ ) (e.g. Dickinson et al., 1987). This difference, captured in second-generation models, provided a major opportunity to begin integrating satellite data into LSMs (e.g. Sellers et al., 1994). Second-generation LSMs also explicitly represented the impact of Vegetation on momentum transfer. Canopies are rough and generate turbulence, which enhances the exchange of H and  $\lambda E$ , and capturing this enhancement was an important step forward.

Second-generation models improved the physical representation of the continental surface and probably the simulation of climate because, along with improvements in the simulation of evaporation, vegetation parameters, etc., they also contained improved soil temperature and soil moisture representations.

It is an open question as to what extent changing a first-generation scheme to a second-generation scheme really improved the simulation of climate. The change between schemes needs for a change in model physics, model parameters and often changes in the host climate model. Although it is not always absolutely clear where subsequent improvements in climate

simulations originate from, Desborough and McAvaney (2001) showed that, as the complexity of the surface energy balance increases in an LSM, the climate does appear to be affected.

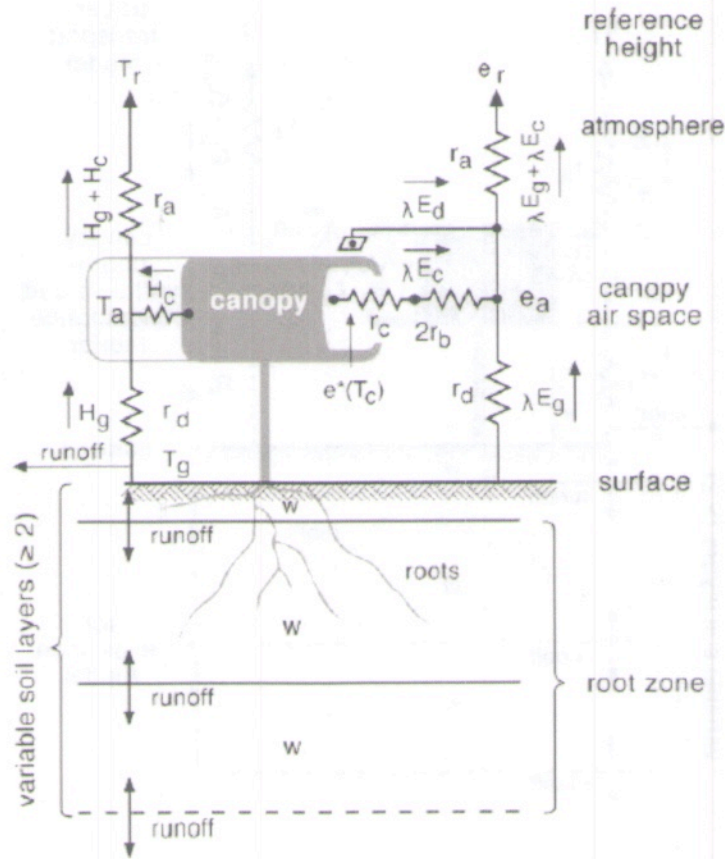


Figure 10 Illustration of a second-generation land surface model. Terms not defined in the text are the reference height for temperature  $T_r$ , the maximum soil moisture capacity ( $W_{max}$ ) and the soil moisture content  $w$ . Modified from (Sellers et al., 1997)

There is evidence strongly suggesting that the second-generation models do improve the modelling of surface-atmospheric exchanges, at least on the time scale of days. Therefore, it was supported by the weather forecasting community to move to second-generation schemes (Pitman, 2003).

### 3.3 THIRD-GENERATION MODELS

The major advance -and major limitation- of second-generation LSMs is that they model canopy conductance empirically, taking into account plant and environmental conditions, but they only use this conductance to model transpiration. It was recognized in the late 1980s that the addition of an explicit canopy conductance provided a means to improve the simulation of the evapotranspiration pathway, as well as to address the issue of carbon uptake by plants. The 'greening' of LSMs represented a major revolution in the modelling capability.

The addition of carbon into LSMs needed the support of the plant physiology community. Third-generation schemes are identifiable by the method used to model carbon. These LSMs

tend to employ representations of other processes (soil temperature, soil hydrology, runoff, ...) that are similar to those included in second-generation LSMs (Figure 11).

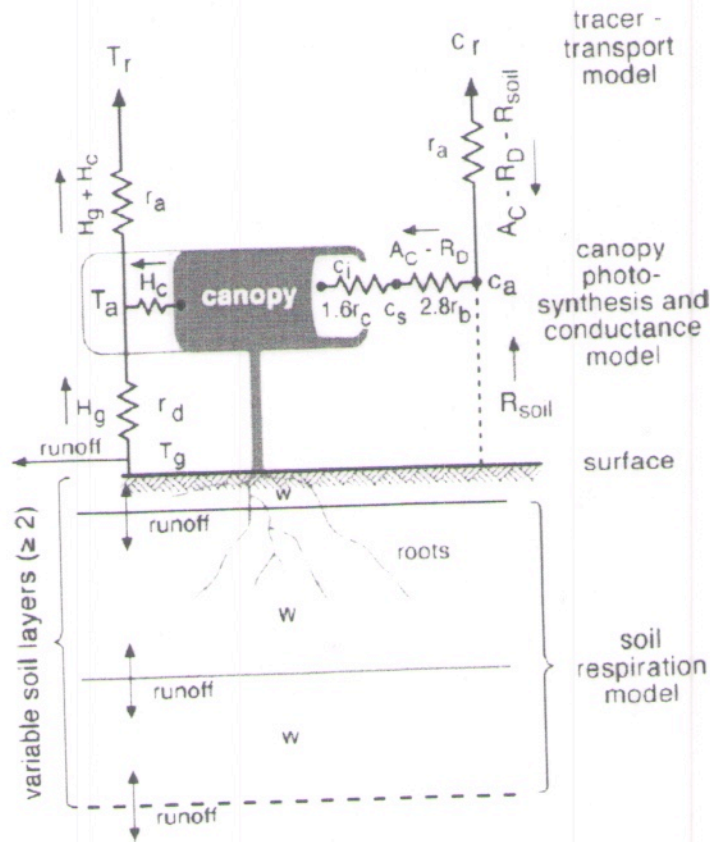


Figure 11 Illustration of a third-generation land surface model. Terms not defined in the text are the reference height for temperature,  $T_r$ , the maximum soil moisture capacity ( $W_{max}$ ) and the soil moisture content  $w$ . Modified from (Sellers et al., 1997)

An LSM that has been able to respond to changes in climate through influencing energy and water exchange (although with largely static vegetation-related characteristics) can now respond in two further ways to a climate change. It can now respond physiologically, as increasing  $CO_2$  influences the canopy conductance and it can respond structurally by growing different leaves or taller trees.

The evolution of the LSMs is represented in the Figure 12, where the increasing levels of detail being added into surface modeling approaches. The second box represents first- and second-generation land surface models. The addition of vegetation phenology (using via semi-mechanistic models of leaf photosynthesis and respiration) defines third-generation models. The allocation of the net carbon balance, and other additions to reflect the full terrestrial carbon cycle translates a 'land surface scheme' into a dynamic global vegetation model DGVM. In each case, the requirements are additive, so that a fully coupled DGVM requires the traditional (usually second-generation) land surface model.

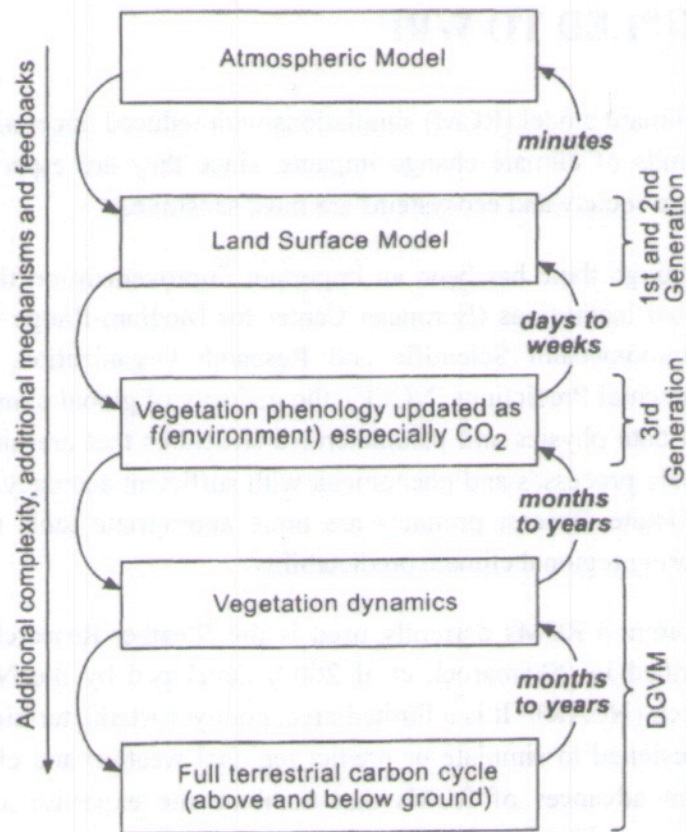


Figure 12 Schematic of the increasing levels of detail being added into surface modeling approaches

## 4 LSMs COUPLED TO WRF

Accurate regional climate model (RCM) simulations with reduced uncertainties are needed to better assess the limits of climate change impacts, since they are especially significant at regional scales, where society and ecosystems are most sensitive.

At the moment, although there has been an important improvement on the regional climate forecasts at the global institutions (European Center for Medium-Range Weather Forecasts, the Australian Commonwealth Scientific and Research Organization, and the National Centers for Environmental Predictions, NCEP), the majority of global climate models usually have oversimplified data physics and parameterized structures that are unable to adequately describe regional-scale processes and phenomena with sufficient accuracy. Therefore, RCMs driven by global climate forecast products are more appropriate tools to overcome these limitations for exploring regional climate predictability.

One of the most common RCMs currently used is the Weather Research, and Forecasting model (WRF, described in (Skamarock et al.,2008) developed by the National Center for Atmospheric Research (NCAR). It is a limited-area, nonhydrostatic, terrain-following sigma-coordinate model designed to simulate or predict regional weather and climate. This model represents the recent advances of RCMs that combine the expertise and experience for mesoscale meteorology and land-surface and climate science developed over the last decades.

The increasingly finer spatial and temporal resolutions and improved PBL parameterizations used in the WRF model (and other mesoscale numerical models) permit us to realistically simulate the diurnal and vertical structure of the PBL. Correctly treating the land surface processes has become really important for the model, since they provide the surface boundary conditions that influence the PBL structure, clouds and precipitation processes. But the initial mesoscale structure at small scales is hardly ever captured by the observational network, and it is necessary for the mesoscale models to include a LSM that properly initializes the state of the ground during a data assimilation period and helps capture the mesoscale structures in the free atmosphere and PBL forced by the ground surface. Such mesoscale circulations are induced by land surface forcing, and depend on topography, soil moisture, surface vegetation and soil characteristics.

Therefore, it is necessary to select an adequate but relatively simple LSM for real-time mesoscale weather and hydrology applications, because the computational time becomes a serious constraint for most such applications. The selection of the LSM is further complicated by the fact that most LSMs require a large number of parameters related to the vegetation and soil state. Another major problem is related to the initialization of soil moisture and temperature fields (Chen and Dudhia,2001). It is not easy to choose between all the possible LSMs to couple to WRF, taking into account their different complexity (see previous sections), computational time, requirements and purpose of the work needed to achieve in any particular case.



It is important to select a relatively simple and sound land surface model, so that it can be efficiently executed for real-time atmospheric and hydrologic applications at different scales. The LSM should be able to provide not only reasonable diurnal variations of surface heat fluxes (which is, of course, the primary function of an LSM), but also correct seasonal evolutions of soil moisture in the context of a long-term data assimilation system. This, in turn, will ensure the accurate partitioning of available surface energy into latent and sensible heating.

The main characteristics of seven possible land-surface options in the WRF model are presented in the following sections. Firstly, each one of them will be reviewed separately (Sections 5-11) and then, they will be compared to one another (Section 12).

## 5 FIVE-LAYER THERMAL DIFFUSION MODEL

The five-layer model is one of the first "second-generation models", following Deardorff (1978), since processes involved in the soil-atmosphere interaction started to be treated explicitly and mathematically, although it uses very simple formulations. Neither runoff nor canopy transpiration processes are considered in this LSM. Snow cover is treated as any other land use category, but there is not a snow scheme. Technical details can be found in (Dudhia, 1989).

The transfer of heat determining soil temperature follows the one-dimensional simple diffusion equation (i.e. the heat flux is linearly proportional to the temperature gradient). The flux convergence is proportional to heating. The parameters that appear in such formulations (soil's thermal diffusivity and specific heat capacity) are constant in time, depending only on the land use category of each grid cell. Available soil moisture is also determined by such classification and remains constant during the whole simulated period. There are two sets of values of soil moisture for each land use category, one for the summer and one for the winter.

This model uses five soil layers with thicknesses, from top to bottom, of 1, 2, 4, 8 and 16 cm. Below the bottom level, at 31 cm, the substrate temperature is kept constant in a 32-cm thick layer. Thus, the maximum soil depth taken into account in this model is 63 cm.

## 6 NOAH MODEL

### 6.1 ORIGIN AND EVOLUTION

At the onset of the 1990s, the National Centers for Environmental Prediction (NCEP) started testing the efficient LSM developed for use in NWP at Oregon State University (OSU) beginning in the middle 1980s (Mahrt and Pan,1984) and (Pan and Mahrt,1987) (see figure 13). The original OSU LSM (first version of the current Noah LSM) consisted of two soil layers with thermal conduction equations for soil temperature and a form of Richardson's equation for soil moisture. The effect of stomatal control by plants was represented via a constant 'plant coefficient' (fractional, 0 to 1) to account for atmospheric influences, multiplied by the soil moisture availability (fractional, 0 to 1) to account for the soil moisture influence, finally multiplied by the potential evaporation (Mahrt and Ek,1984). Later on a variable plant coefficient that accounted for stomatal control was related to a canopy conductance formulation using the common 'big leaf' approach (Noilhan and Planton,1989), where canopy conductance is modeled as a function of soil moisture availability and atmospheric conditions (solar insolation, temperature, and humidity).

Date	Description	Reference(s)
	<i>Original OSU LSM (Prior to NCEP Era)</i>	
	potential evaporation	Mahrt and Ek [1984]
	surface fluxes, soil hydraulics, and soil thermodynamics	Mahrt and Pan [1984] and Pan and Mahrt [1987]
	<i>Noah LSM Implementation in Eta Model at NCEP</i>	
31 Jan. 1996	OSU LSM introduced into Eta model (GFS initial soil moisture and temperature)	Chen et al. [1996]
24 July 1996	surface runoff and infiltration	Schaake et al. [1996]
18 Feb. 1997	ISLSCP vegetation greenness changes	Gutman and Ignatov [1998]
	NESDIS vegetation greenness	Betts et al. [1997]*
	bare soil evaporation changes	Betts et al. [1997]*
	snow melt changes	F. Chen et al. [1997]*
9 Feb. 1998	thermal roughness length changes	
3 June 1998	increase from 2 to 4 soil layers	
	self-cycling Eta-EDAS soil moisture and temp.	
	NESDIS daily snow cover and sea ice analysis	Ramsay [1998]
	<i>Noah LSM Upgrades (With Assessment in Eta Model) Described in This Study</i>	
21 July 2001	frozen soil physics	Koren et al. [1999]
	snowpack physics upgrade	Koren et al. [1999]
	maximum snow albedo climatology	Robinson and Kukla [1985]
	shallow snow thermal conductivity	Lunardini [1981]
	bare soil evaporation refinement	
	bare soil thermal conductivity changes	Peters-Lidard et al. [1998]
	vegetation-reduced soil thermal conductivity	Peters-Lidard et al. [1997]
	transpiration refinements	
26 Feb. 2002	patchy shallow snow thermal conductivity	

Figure 13 Timeline of the Noah Landsurface Model evolution with references to relevant Model Physics and/or Land Surface fields implemented in the NCEP operational Mesoscale Eta Model (Ek et al., 2003)

During the 1990s, NCEP greatly expanded its land surface modeling collaborations via several components of the Global Energy and Water Cycle Experiment (GEWEX), most notably, the GEWEX Continental-scale International Project (GCIP) and the Project for Inter-comparison of Land-surface Parameterization Schemes (PILPS). These collaborations included the Office of Hydrological Development (OHD) of the National Weather Service, National Environmental Satellite Data and Information Service (NESDIS), NASA, National Center for Atmospheric Research (NCAR), the U.S. Air Force, and OSU and other university partners. As an outgrowth of these collaborations and their broad scope of LSM testing in

both uncoupled and coupled mode over a wide range of space scales and timescales, NCEP substantially enhanced the OSU LSM, now renamed the Noah LSM in recognition of the broad partnership above (Ek et al.,2003).

It can be said that the Noah model was based on coupling of the diurnally dependent Penman potential evaporation approach of (Mahrt and Ek,1984), the multilayer soil model of (Mahrt and Pan,1984), and the primitive canopy model of (Pan and Mahrt,1987).This model was extended with a canopy resistance formulation and a surface runoff scheme by (Chen et al.,1996) and implemented into the MM5 and WRF model for the model coupling system. Some improvements on this configuration, through vegetation parameterization and soil moisture data initialization on a regional scale using remote sensing data and a land data assimilation system, are shown in (Hong et al.,2009).

The Noah model can be considered as a “second-generation” model (see Section3), since processes involved in the soil-atmosphere interaction is treated explicitly and mathematically. It cannot yet be considered a “third-generation” model, since it does not include dynamic considerations for vegetation and other issues, as it will be explained in Section 7.

## **6.2 MODEL CHARACTERISTICS**

### **6.2.1 SOIL AND CANOPY LAYERS**

For the soil model to capture the daily, weekly and seasonal evolution of soil moisture and also mitigate the possible truncation error in discretization, the soil is divided into four layers, with increasing thickness toward the bottom, of 0.1, 0.3, 0.6 and 1m (Figure 14) . The total soil depth considered in the model is 2m, with the root zone in the upper 1m of soil. Thus, the lower 1-m soil layer acts like a reservoir with gravity drainage at the bottom. The depth of the vegetation roots can be specified as a function of vegetation type, if realistic rooting-depth data are available. The temperature at the lower boundary (assumed to be 2 m below the ground surface) is kept constant over time.

The model has also one canopy layer being, at the beginning, a combined vegetation-soil surface, and later separated, following the Pan and Mahrt scheme (Pan and Mahrt,1987), although no fluxes canopy-soil are considered. The prognostic variables are: soil moisture and temperature in the soil layers, water stored on the canopy, and snow stored on the ground.

### **6.2.2 DIFFUSIVITY AND THERMODYNAMICS**

The ground heat flux is controlled by the thermal diffusion equation for soil temperature and heat transport (Chen and Dudhia,2001), but in this model heat capacity and thermal conductivity are formulated as functions of the soil water content, and depend on both land use and soil type categories.

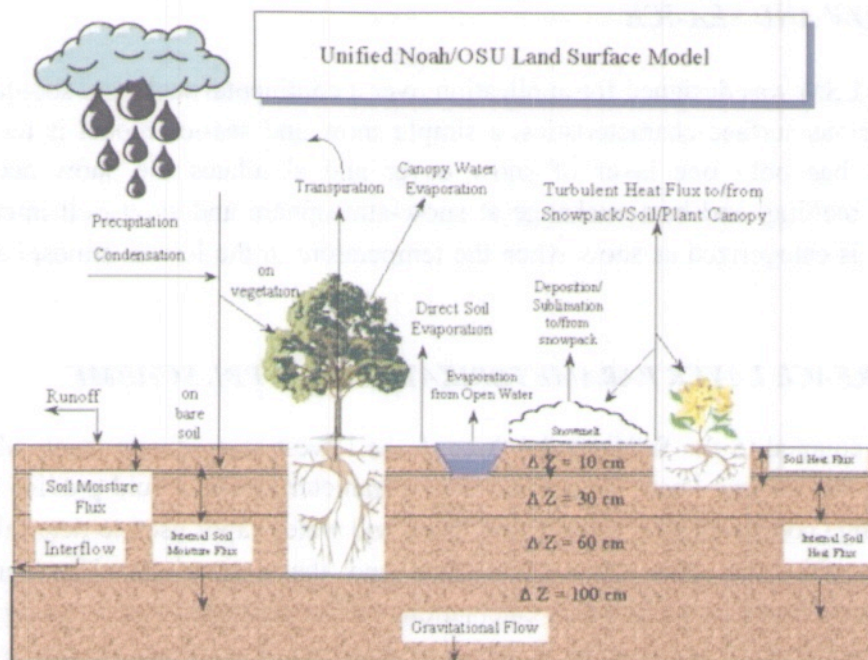


Figure 14 Schematic representation of the Noah LSM

The diffusivity is taken from of Richards' equation for simulating the soil moisture content, where the hydraulic conductivity and the soil water diffusivity are also functions of the soil water content (Mahrt and Pan, 1984) and (Pan and Mahrt, 1987). Sources and sinks are taken into account, i.e. direct precipitation, superficial and underground runoff, direct evaporation and plant transpiration. The total evaporation has three contributions: direct evaporation from the top shallow soil layer, evaporation of the precipitation intercepted by the canopy, and transpiration via canopy and roots. The vegetation fraction ( $Fg$ )<sup>3</sup> is taken into account in these formulations. The surface skin temperature is determined following (Mahrt and Ek, 1984) by applying a single linearized surface energy balance equation representing the vegetation surface.

### 6.2.3 HIDROLOGY

A surface runoff model is adopted in the Simple Water Balance (SWB) model to calculate the surface runoff. The SWB model (Schaake et al., 1996) is a two-reservoir hydrological model that is typically calibrated for large river basins and that takes into account the spatial heterogeneity of rainfall, soil moisture, and runoff. The soil-snow-vegetation system is represented as a single heat/water vapor source in Noah for the computation of surface energy and water budgets. A diurnal Penman approach (Mahrt and Ek, 1984) linked to a modestly complex canopy resistance scheme (Chen et al., 1996) is utilized for simulating the evapotranspiration.

<sup>3</sup>  $Fg$  is defined as the percentage or fraction of occupation of vegetation canopy in a given ground area in vertical projection

#### 6.2.4 SNOW AND SEA-ICE

Because this LSM was designed for application over a continental scale and should be able to deal with various surface characteristics, a simple snow and sea-ice model is included. The snow model has only one layer of snow cover and simulates the snow accumulation, sublimation, melting, and heat exchange at snow-atmosphere and snow-soil interfaces. The precipitation is categorized as snow when the temperature in the lowest atmospheric layer is below 0°C.

#### 6.2.5 SURFACE LAYER PARAMETERIZATION AND PBL SCHEME

The LSM is coupled to the WRF model through the lowest atmospheric level, which is also referred to as the surface layer. A surface layer parameterization should provide the surface (bulk) exchange coefficients for momentum, heat, and water vapor used to determine the flux of these quantities between the land surface and the atmosphere. The surface layer parameterization bases its surface flux calculations on the similarity theory, using a stability-dependent function ( $\psi_h$ ) and roughness length to determine the surface exchange coefficient for heat and moisture (Chen and Dudhia,2001) . The LSM essentially replaces the WRF ground temperature prediction calculation that was based on the energy budget at the ground.

#### 6.2.6 LAND SURFACE CHARACTERISTIC FIELDS AND PARAMETER SPECIFICATION

In the coupled WRF-LSM system, the secondary vegetation and soil properties such as albedo, minimum stomatal resistance<sup>4</sup>, and soil thermal/hydraulic conductivity are determined by the spatial distribution of vegetation and soil types. There are two primary variables upon which other secondary parameters (such as minimal canopy resistance and soil hydraulic properties) are determined: one is the vegetation type, using the 1-km resolution U.S. Geological Survey's (USGS) vegetation categorization, which used to include 16 land cover classes. It would be classified in 19 categories in later versions; the other one is the soil texture, determined by using the 1-km resolution multilayer 16-category soil characteristics dataset based on the U.S. Department of Agriculture's State Soil Geographic Database (USDA), in the earlier versions. It currently can use either the 24 USGS or the 20 MODIS classes.

As it was said above, the green vegetation fraction ( $F_g$ ), plays a very important role in the determination of the evapotranspiration (ET) components. However, the  $F_g$  parameter used in the earlier versions of the Noah LSM (Chen and Dudhia,2001) came from 5 years' worth of monthly Advanced Very High Resolution Radiometer (AVHRR) data (1986-1991) with 0.15° of spatial resolution, which is about 15 km in Central America. Considering that one of the merits of the recently advanced WRF model is to provide simulations with very high

---

<sup>4</sup> The opposition to transport of quantities such as water vapor and carbon dioxide to or from the stomata (pores) on the leaves of plants.

resolution of 1 km or higher, the Fg parameter in the coarser resolution may negatively affect model accuracy and reliability for finer scale simulations. In terms of temporal resolution, monthly Fg data was not able to provide enough information to describe short-term variations of land cover such as weekly or biweekly periods.

That is why some improvements were made in the model. In order to test the model improvement and reliability on Fg parameterization with better vegetation observation data, Hong et al.(2009) applied two different Fg derivation methods to the model parameterization. The two derivation methods utilized satellite derived Normalized Difference Vegetation Indices (NDVI) from Moderate Resolution Imaging Spectroradiometer (MODIS) surface reflectance.

### **6.2.7 INITIALIZATION OF SOIL MOISTURE**

The initialization of soil moisture in coupled regional models was jeopardized by the fact that there was no routine soil moisture observation. Thus, until a soil moisture data assimilation system was developed for the WRF, the initialization of the LSM largely depended on soil moisture fields obtained from analysis /forecasts from other models.

Even though proper soil moisture initialization from field observation data for several locations resulted in reasonable simulations of soil moisture variations, latent heat simulations responded very sensitively to those variations, showing overestimations when soil moisture and vegetation were relatively high.

### **6.2.8 IMPROVEMENTS IN THE NOAH MODEL**

Recently, there have been some improvements trying to mitigate the errors due to the lack of proper soil moisture data assimilation, assimilating the estimates from the National Aeronautics and Space Administration (NASA) Soil Moisture Active Passive (SMAP) radiometer (Blankenship et al.,2018).

Different new physics options for the Noah model have been added in order to avoid some issues in the model. For instance, (Zheng et al.,2016) have validated some of these options for the source region of the Yellow River (SRYR) in order to investigate their ability in reproducing runoff at the catchment scale. Three sets of augmentations are implemented affecting descriptions of (i) turbulent and soil heat transport (Noah-H), (ii) soil water flow (Noah-W), and (iii) frozen ground processes (Noah-F). Five numerical experiments are designed with the three augmented versions, a control run with default model physics and a run with all augmentations (Noah-A).

These improvements and options in the Noah model led to the development of a new model, the Noah-MP (multi-parameterization), which will be described in the following section.

## 7 NOAH-MP MODEL

### 7.1 ISSUES IN THE NOAH LSM

The Noah model version 3.0 (V3) had a combined surface layer of vegetation and soil surface, over which surface energy fluxes were computed. Such a model structure impeded its further development as a process-based dynamic leaf model, because it cannot explicitly compute photosynthetically active radiation (PAR), canopy temperature, and related energy, water, and carbon fluxes. Noah has a bulk layer of snow and soil. For a thick snowpack, such a layer structure tends to underestimate the ground heat flux because of the combined thickness of snowpack and half of the top-layer soil, leaving too much energy at the snow surface and being thus too prone to snowmelt.

Additionally, percolation, retention, and refreezing of melt liquid water cannot be readily represented in such a layer structure. Noah has a total soil depth of two meters and uses gravitational free drainage at the model bottom as the lower boundary condition of soil moisture. Drained water from the 2 m soil bottom should accumulate in its underlying soil or aquifer during wet seasons when recharge rate exceeds discharge rate and, driven by capillary forces, be able to be drawn back to the 2 m soil column in dry seasons. Noah's shallow soil column is not able to capture the critical zone (down to 5 m) to which the surface energy budgets are most sensitive. Immediate removal of the drained water (due to the free drainage scheme) in Noah may result in too short memories of antecedent weather events or climate anomalies. The impeding effect of frozen soil on infiltration and further effects on river discharge is evidently weaker than that represented in most current LSMs. The frozen soil in Noah is too impervious under most vegetation and climate conditions, resulting in too much surface runoff in spring or early summer and, hence, less infiltration of snow-melt water into soil (Niu et al., 2001a) and (Niu et al., 2001b).

### 7.2 TRANSITION FROM THE NOAH LSM TO THE NOAH-MP LSM

The Noah model has been tested through a number of tests and different issues have been pointed out that need to be solved (see Section 6.2.8). Thus, there have been great efforts in improving the Noah LSM through mathematical formulations, augmenting conceptual realism in biophysical and hydrological processes. The enhanced conceptual realism includes (1) the vegetation canopy energy balance, (2) the layered snow-pack, (3) frozen soil and infiltration, (4) soil moisture-groundwater interaction and related runoff production, and (5) vegetation phenology (Figure 15). In (Niu et al., 2001b), ensemble evaluations with long-term regional (basin) and global scale data sets were performed.

It is promising that multi-model averages resulted in generally better behavior. Therefore, it is necessary to develop an LSM that accommodates numerous combinations of parameterization schemes for an ensemble representation of processes in nature. The model with multiple parameterization options has a great potential to facilitate (1) physically based ensemble



climate predictions, (2) identification of the optimal combinations of schemes and explanation of model differences, and (3) identification of critical processes controlling the coupling strength (Koster and Suarez, 1992) between the land surface and the atmosphere.

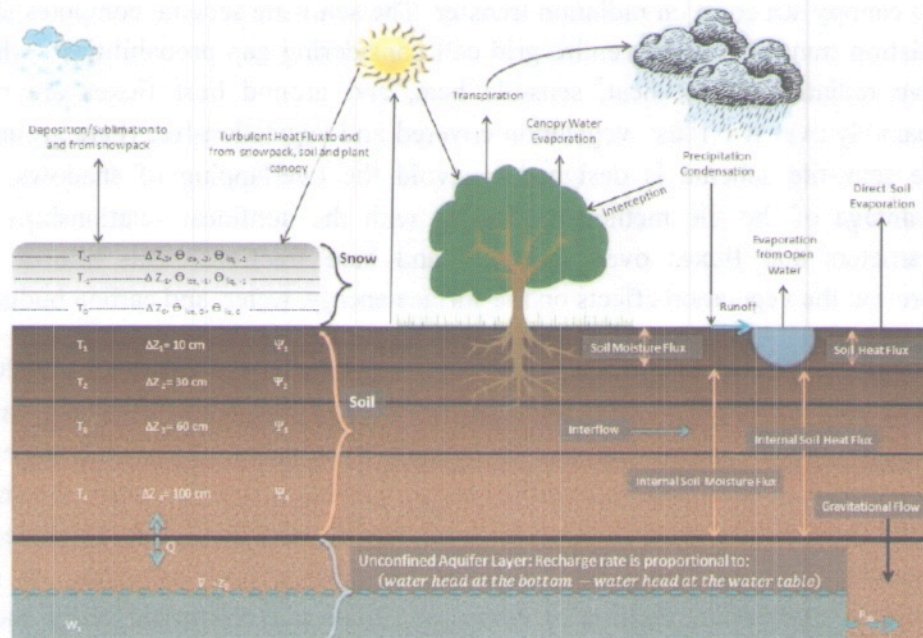


Figure 15 Schematic representation of the Noah-MP LSM

The baseline model of Noah-MP is the Noah LSM model because it is coupled with the Weather Research and Forecast (WRF) model that provides multi-options for atmospheric physical processes. For instance, the Noah LSM is known to have biases in simulating runoff and snow-melt. Thus, there is an increase of its representations of hydrological processes and surface energy fluxes that affect the hydrological processes. The Noah LSM has a combined surface layer of vegetation and snow (when snow covers the soil surface), impeding an accurate prediction of snow skin temperature and thus, snow-melt. In Noah-MP the vegetation canopy is separated from the ground and then added various hydrological schemes. The augmentations are complex and comprehensive including the structural change.

### 7.3 MAIN AUGMENTATIONS TO THE NOAH LSM

The most important augmentations to the Noah LSM are:

- A separated vegetation canopy layer to compute the canopy and the ground surface temperatures separately. This layer is defined by a canopy top and bottom with leaf physical and radiometric properties.
- A modified two-stream canopy radiation transfer scheme. The two-stream radiation scheme (Sellers, 1985) computes Solar zenith angle (SZA)-dependent fluxes that are reflected by the surface, absorbed by the canopy, and absorbed by the ground over two wave bands: visible and near-infrared. The scheme accounts for scattering and

multiple reflections by the canopy and ground in two mainstreams of radiative fluxes: vertical upward and downward. However, it assumes that the canopy leaves are evenly distributed within a grid cell. A 'semi-tile' subgrid scheme was developed to account for the effects of vegetation canopy gaps varying with Solar zenith angle (SZA) and the 3-D canopy structure on radiation transfer. The semi-tile scheme computes shortwave radiation transfer over the entire grid cell considering gap probabilities, while long-wave radiation, latent heat, sensible heat, and ground heat fluxes are computed separately over two tiles: vegetation-covered and vegetation-free (bare ground) areas. The semi-tile scheme is designed to avoid the overlapping of shadows and take advantage of the tile method in dealing with the nonlinear relationships between parameters and fluxes over vegetated and bare fractions. This allows to better represent the vegetation effects on the surface energy, water, and carbon budgets.

- A three-layer snow model and a snow interception model (Niu and Z.L.,2004) was added into the Noah model. Because the interception capacity by the canopy for snowfall is much greater than that for rainfall, interception of snowfall by the canopy and subsequent sublimation from the canopy snow may greatly reduce the snow mass on the ground. The model allows for both liquid water and ice to be present on the vegetation canopy. The model accounts for loading and unloading of snowfall, percolation, retention, melting of intercepted snow and refreezing of the melt-water, frost/sublimation, and dew/evaporation.
- A more permeable frozen soil was introduced into the Noah LSM by separating a grid cell into permeable and impermeable fractions.
- A simple groundwater model, that is a revised version of that by (Niu and Z.L.,2007) was added into the Noah model. Below the 2 m bottom of the Noah soil column, an unconfined aquifer was added to account for the exchange of water between the soil and the aquifer. A simple TOPMODEL-based runoff model (Niu et al.,2005) was added to compute surface runoff and ground-water discharge, which are both parameterized as exponential functions of the depth to water table. model with a TOPMODEL-based runoff scheme.
- A short-term dynamic vegetation model, which requires photosynthetically active radiation (PAR), photosynthesis, and leaf temperature for sunlit and shaded leaves. It allows to predict the leaf area index (LAI) and the green vegetation fraction (Fg).

On the basis of the augmented Noah LSM, there are designed optional schemes for dynamic vegetation, stomatal resistance, the drought stress factor, runoff, radiation transfer, aerodynamic resistance, snow surface albedo, super-cooled liquid water in frozen soil, frozen soil permeability, and partitioning precipitation into snowfall and rainfall. Horizontal and vertical vegetation density can be prescribed or predicted using prognostic photosynthesis and dynamic vegetation models that allocate carbon to vegetation (leaf, stem, wood and root) and soil carbon pools (fast and slow). It is because of all of these augmentations, that the Noah-

MP model can be considered a 'third-generation' model and it starts to show some advantages of the Dynamic global vegetation models (see Section 3).

In the WRF model version 3.9, some urban physics was also added to the Noah-Mp LSM. It was also added a groundwater model and crop-related input data. It adds four additional variables: crop type, planting, harvest and climatological growing degree days over crop season.

## 8 RAPID UPDATE CYCLE MODEL (RUC)

### 8.1 MODEL OVERVIEW

The NOAA Rapid Update Cycle (RUC) is a mesoscale atmospheric data analysis and prediction system configured with a hybrid isentropic-sigma vertical coordinates and run operationally at the National Centers for Environmental Prediction (NCEP). Unlike the other LSMs described in this document, the RUC model is an atmospheric model itself that includes a land surface parameterization, although this parameterization can also be used by other atmospheric models, like the WRF model. That is why an introduction about the main characteristics of the model will be presented, followed by the description of the modifications in the land surface parameterization to use in the WRF model.

Primary users include the aviation, severe weather, and general forecast communities, including National Weather Service Forecast Offices. The RUC is unique among operational numerical weather prediction (NWP) systems in two primary aspects: its hourly forward assimilation cycle, and its use of a hybrid isentropic/terrain-following vertical coordinate for both its assimilation and forecast model components (Benjamin et al., 2004b) and (Benjamin et al., 2004a). It is distinguished from other hybrid isentropic forecast systems by its application at a fairly high horizontal resolution (10-20 km).

Within the 3DVAR analysis, the use of the quasi-isentropic coordinate system for the analysis increments allows the influence of observations to be adaptively shaped by the potential temperature structure around the observation. The use of entropy as a vertical coordinate has a strong conceptual appeal, since it was recognized that the entropy of dry air is monotonically increasing with height as viewed from a synoptic-scale perspective. Apart from their dynamical appeal, isentropic-coordinate models are potentially advantageous in that they reduce (or eliminate, in the case of adiabatic flow) cross-coordinate vertical transport through coordinate surfaces. In these models, lateral mixing is carried out on isentropic surfaces rather than across them, meaning that no unwanted cross-isentropic mixing occurs.

Isentropic coordinates are also advantageous in that they provide adaptive vertical resolution, greater in layers of higher static stability where strong vertical gradients of other variables are likely to occur. The concentration of isentropies in frontal zones of high thermal contrast means that these zones appear as larger-scale features in both along-front and cross-front dimensions when viewed in an isentropic perspective (e.g., Benjamin, 1989).

### 8.2 MODEL PHYSICS

The dynamical equations and their finite-difference approximations that form the basis for the RUC model are given in (Benjamin et al., 2004b). In addition to the horizontal momentum equations, the hydrostatic equation, the equation for continuity of mass, and the first law of thermodynamics, there are budget equations with source and sink terms for the mixing ratios of water vapor and each of the five hydrometeor species (cloud and rain water, cloud ice,

snow and graupel) and the number concentration of cloud ice. There is no vertical staggering of variables; only the mass continuity is applied to the layer between adjacent hybrid-isentropic coordinate surfaces.

Despite possible issues -as for example inaccuracies in vertical cross-coordinate transport due to use of a non-staggered vertical grid- the hybrid  $\theta$ - $\sigma$  RUC model has been shown to reduce vertical dispersion caused by cross-coordinate vertical transport compared to quasi-horizontal models, and thereby to improve numerical accuracy for moist reversible processes. It produced an accurate forecast with sharply defined 3-D dynamical and moisture structures for a case study at 20-km resolution.

The RUC is a full-physics model, that is, it contains parameterizations or representations of the main physical processes that involve subgrid vertical transports or processes that are too complicated to be described explicitly. In the 2003 version of the RUC20 (Benjamin et al., 2004a and 2004b) these were as follows:

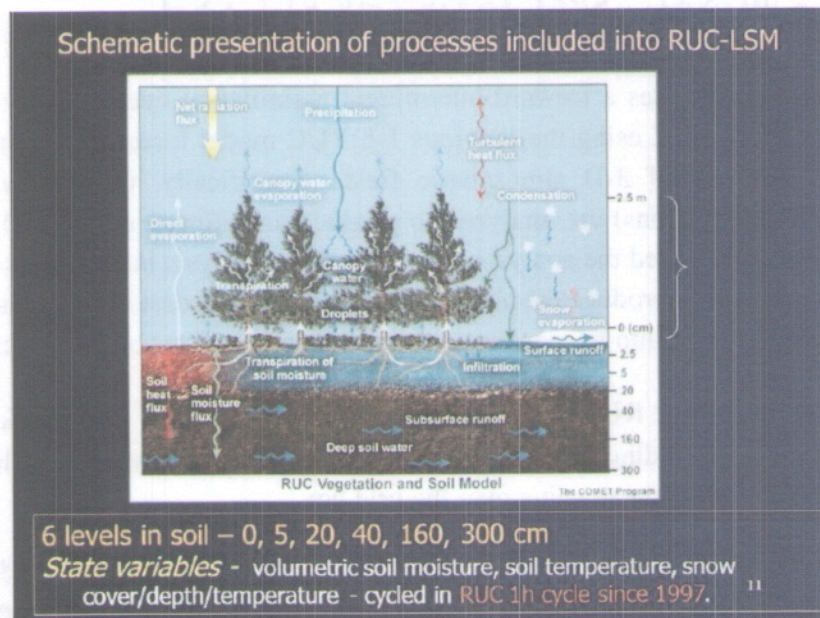


Figure 16 Schematic representation of the RUC LSM

- Short-wave radiation: Dudhia (1989) broadband with attenuation by  $O_3$  and attenuation/reflection by grid-scale clouds.
- Long-wave radiation: Dudhia (1989) broadband including absorption and reemission by clouds.
- Land surface and surface fluxes: Smirnova et al. (1997 and 2000) including two-layer snow, 6-layer soil and cycling of snow cover and snow water equivalent as well as soil temperature and moisture (Figure16).

- Subgrid turbulent vertical mixing: Pan et al.(1994) in surface layer, modified Burk-Thompson in 1989 (based on Mellor-Yamada level 2) above the surface (including upper levels).
- Convection: Grell and Devenyi (2002) ensemble-closure scheme.
- Grid-scale microphysics: mixed-phase bulk microphysics scheme used in the MM5 model (Thompson et al., 2004) with explicit forecast of mixing ratios of cloud water, rain, cloud ice, snow, graupel, and cloud-ice number concentration, as well as diagnosis of variable number concentration for rain and snow.

These schemes are summarized in (Benjamin et al.,2004b) and described in more detail in the cited references. In addition to the coupling between the schemes noted above, parameterized convection is a source term for grid-scale cloud water or cloud ice (depending on temperature) that is processed by the grid-scale microphysics.

### **8.3 OPERATIONAL ASPECTS OF THE RUC LSM**

The Rapid Update Cycle uses a forward intermittent assimilation cycle. Every hour, recent observations are assimilated using the previous 1-h RUC model forecast as a background to produce a new estimate of 3-D atmospheric fields. Specifically, the observation-minus-forecast residuals (innovations) are analyzed to produce an estimate of the 3-D multivariate forecast error field, also called the analysis increment. This analysis increment is added to the 1-h forecast background to produce the new analysis. The 1-h forecast contributes information from previous observations into the current analysis through the filter of the forecast model.

The surface elevation of the RUC is defined using a slope envelope. The standard envelope topography is defined by adding the subgrid-scale terrain standard deviation (calculated from a 10-km terrain field) to the mean value over the grid box.

In addition to topography, there are other surface fields required by the RUC model, including land use (needed for surface roughness and albedo), vegetation fraction, soil type and rooting depth (all used by the land-surface scheme), and sea- and lake-surface temperature. Most of these fields are the same as used by the EDAS (Eta Data Assimilation System).

### **8.4 MODIFICATIONS IN THE WRF VERSION**

Although the land surface model used in the RUC (RUC LSM) was originally developed to provide more accurate lower boundary conditions for the hourly updated NOAA Rapid Update Cycle (RUC) model, focusing on short-range aviation and severe weather prediction (Benjamin et al., 2004b), it was later extended to wider geographical application (Smirnova et al., 2016). These applications include the Weather Research and Forecasting (WRF) Model (Skamarock et al., 2008) and the NOAA hourly updated Rapid Refresh (RAP; Benjamin and Coauthors,2016) and High-Resolution Rapid Refresh (HRRR; Smith et al.,2008) models.

As a first step, a simple sea ice treatment and further snow component enhancements were added to the RUC LSM. Later, vertical resolution in the soil domain was increased to have nine levels instead of six to improve the diurnal cycle near the surface. These enhancements to RUC LSM are showed in the Figure17 and better described below.

As it was said above, the RUC LSM contains heat and moisture transfer equations, together with energy and moisture budget equations for the ground surface, and uses an implicit scheme for computing the surface fluxes (Smirnova et al., 1997). The energy and moisture budgets are applied to a thin layer spanning the ground surface and consider the heat capacities and densities of both the soil/snow and the atmosphere. The version of this model, tested in 1D off-line tests and implemented in the first version of the RAP model, had six prognostic soil levels, ranging from the soil surface to 300cm in depth (0, 5, 20, 40, 160, and 300 cm). The version in the WRF repository (version 3.4.1 since 2012; Figure17) used in the operational RAPv2 (Benjamin and Coauthors, 2016) uses nine prognostic soil levels (0, 1, 4, 10, 30, 60, 100, 160, and 300 cm), with the highest vertical resolution near the surface (top layer of 1 cm). The thinner top soil layer with nine levels provides a stronger diurnal cycle. The smaller cold bias in daytime and warm bias at nighttime results from use of the nine-level LSM compared to that with the six-level LSM.

RUC LSM characteristics	Smirnova et al. (2000)	WRF version 3.6, 2014
Prognostic vertical levels	Soil = 6 levels (0, 5, 20, 40, 160, 300 cm), snow = 2 levels	Soil = 9 levels (0, 1, 4, 10, 30, 60, 100, 160, 300 cm), snow = 2 levels
Sea ice model	None	Heat diffusion; snow on ice
Snow model	Two-layer snow model, snow area trimming	Two-layer snow model with improvements in snow melting algorithm, snow area trimming/building
Snow melting	Single-iteration energy budget	Two-iteration energy budget
Snow albedo	Constant value (0.75)	Clear-sky maximum surface albedo of snow-covered land computed from DMSP imagery, temperature dependence
Land-use classification	USGS categories	MODIS IGBP-modified categories
Vegetation fraction, LAI	0.144° resolution AVHRR vegetation fraction, no LAI	1-km resolution MODIS FPAR/LAI data;
Surface parameters	Look-up tables for dominant category	Subgrid-scale heterogeneity, includes seasonal variations

*Figure 17 Modifications to the RUC LSM implemented in the WRF version 3.6 model (2014) compared to its predecessor 2000 version. Abbreviations: MODIS 5 Moderate Resolution Imaging Spectroradiometer; FPAR 5 fractional photosynthetically active radiation; IGBP 5 International Geosphere-Biosphere Programme; AVHRR 5 Advanced Very High Resolution Radiometer; LAI 5 leaf area index; DMSP 5 Defense Meteorological Satellite Program*

The RUC LSM has a snow model with one or two additional snow levels depending on snow depth (threshold in 7.5cm.) and a simple parameterization of the processes in frozen soil and treatment for sea ice (Smirnova et al., 2000). It includes changing snow density (compaction parameter) depending on snow depth temperature. Snow can be melted from the top and bottom of snow pack. There is also a prescribed amount of liquid water (13%) from melting that stay inside the snow pack and there is a treatment of mixed phase precipitation. There are two iterations in melting algorithm, time dependent snow/ice albedo. Melted water infiltrates into soil and forms surface runoff. Besides, falling snow can be intercepted by the vegetation canopy until the holding capacity is exceeded.

Surface parameters such as aerodynamic-roughness length, leaf area index, and emissivity are specified based on the dominant vegetation category for the model grid box, as gridded by the WRF Preprocessing System (WPS). WPS extracts the dominant land-use category and fractional land-use data on specific model grids from a global dataset with 30" horizontal resolution. By default, the WPS program uses AVHRR-based USGS data, and these data were also utilized during the early stages of RAP model development and in the first version of the operational RAP at NCEP. However, later an alternative dataset was added to WPS options, based on the Moderate Resolution Imaging Spectroradiometer (MODIS)-derived classification of land surface properties, providing more up-to-date land surface cover over its predecessor, the USGS land-use classification scheme used in the RUC model.

The improved RUC LSM also utilizes higher-resolution MODIS fractional photosynthetically active radiation (FPAR) and leaf area index (LAI) datasets to specify vegetation fraction and leaf area index (applied in RAP and HRRR). The RUC LSM has also new capability to specify land surface parameters as area-weighted averages in the grid box.

This model could be considered to belong to the "second-generation" group in the Land Surface model evolution classification (see Section 3), but currently introducing some processes (like FPAR) more typical of the "third-generation" group.



## **9 PLEIM AND XIU MODEL (PX)**

### **9.1 MODEL OVERVIEW**

The Pleim-Xiu model builds off of the one dimensional prototype (Noilhan and Planton,1989) and later developed in a three dimensional model. The model consists of: a land surface model (ISBA model, Jacquemin and Noilhan, 1990) for the prognostic simulation of soil moisture and soil temperature based on the Interactions between Soil, Biosphere, and Atmosphere; a nonlocal closure PBL model developed by Pleim and Chang (Pleim and Chang,1992) for the simulation of vertical turbulent transport of heat, moisture, and momentum; a flux-profile algorithm that couples the surface with the atmosphere through the surface fluxes, and a simple radiation model (Pleim and Xiu,1995).

### **9.2 SOIL MOISTURE AND THERMODYNAMICS**

There are three pathways for evaporation in the PX LSM: soil surface, canopy, and evapotranspiration. This model simulates the evolution of soil moisture and temperature in two layers, a thin (1-cm thick) surface layer, and a 1-m deep reservoir layer. The zero flux condition is imposed at the bottom, for both temperature and moisture content prognostic algorithms.

Ground surface temperature is computed from the surface energy balance using a force-restore algorithm for heat exchange within the soil. In this LSM, a canopy shelter factor is used to account for shading within denser canopies. Soil moisture coefficients used in the prognostic soil moisture equations are formulated in terms of basic soil parameters such as field capacity, wilting point, saturation, and other thermal and hydraulic properties of the soil. Stomatal conductance is parameterized according to root-zone soil moisture, air temperature and humidity and photosynthetically active radiation (PAR).

### **9.3 SOIL PARAMETERS**

All soil properties are specified according to soil types. Soil parameters are computed from fractional soil texture data. Representative values of surface roughness length used in this LSM are aggregated to the grid cell using the 1-km data for these parameters and the weighted techniques when the model horizontal spacing is larger than 1 km x 1 km grid cell. Similarly, other surface soil parameters as albedo, are computed from fractional soil texture data.

The soil texture data are based on the conterminous U.S. 1-km soil texture datasets for the area within the lower 48 states in the United States, and the Digital Soil Map of the World for other areas (Xiu and Pleim,2001). The base datasets are the USDA State Soil Geographic Database, and the soil maps are generated from detailed soil survey data. The data contain soil texture type according to the USDA soil textural classification (Clapp and Hornberger, 1978) in 11 soil types. The Digital Soil Map of the World is generated by the Food and Agriculture

Organization of the United Nations Educational, Scientific, and Culture Organization. This dataset has three textural classes (coarse, medium, and fine) for map unit polygons of approximately  $1^\circ$  resolution, which we translate into the USDA soil texture classification. Soil texture-related parameters such as saturation  $w_{sat}$ , field capacity  $w_{fc}$ , and wilting point  $w_{wilt}$  are defined according to the USDA classification following the ISBA model (Jacquemin and Noilhan, 1990).

#### 9.4 VEGETATION PARAMETERS AND TYPES

Similarly, the vegetated land use attribution at each grid cell is perceptual. Grid-cell representative values of vegetative parameters, such as leaf area index (LAI), vegetation coverage, albedo, and minimum stomatal resistance, are computed by the PX model using the fractional land use data. For technical details see (Xiu and Pleim, 2001).

The land use-related parameters are derived from the North American Land Cover Characteristics Database available from the U.S. Geological Survey (USGS), which is based on 1-km Advanced Very High Resolution Radiometer data. These data are available in the USGS Land Use-Land Cover (LULC) System (Anderson et al., 1976), often referred to as Anderson level 2, which is composed of 24 vegetation/land use types. Land use-related parameters as specified for 24 vegetation/land use types.

In this model, a possible alternative to using LAI to estimate the relationship between stomatal and canopy conductance is to use remote sensing data such as the normalized difference vegetation index (NDVI), which can be derived directly from satellite data. This idea is attractive for two reasons: 1) NDVI accounts for the shading effects in dense canopies better than LAI does with an empirical shelter factor because NDVI is derived from a 'bird's-eye' view of the canopy; and 2) NDVI gives a realistic estimate of seasonal changes in vegetative cover, thereby obviating the need for seasonal vegetation parameterizations.

#### 9.5 SNOW TREATMENT

The PX LSM currently does not contain a process to account for the accumulation, sublimation, or melting of snow (Gilliam and Pleim, 2009). Rather, it uses 3-hourly gridded snow-water equivalent from the National Centers for Environmental Prediction (NCEP) North American Mesoscale model (NAM) analysis for snow cover. It has been noted in past evaluations (i.e., Gilliam et al., 2006) that the PX LSM does not perform as well as some other land surface models over snow. Several improvements for snow cover were made in the PX LSM including an updated volumetric heat capacity for snow and a fractional snow coverage that is a function of land use and snow depth, following the method used in the Noah land surface model (Ek et al., 2003). The fractional snow coverage is then used by the PX LSM to compute a weighted surface heat capacity and albedo, which have a significant impact on ground heating and cooling rates.

## 9.6 DATA ASSIMILATION

Without a sophisticated method for soil moisture initialization and/or some kind of soil moisture nudging scheme, the addition of an LSM usually degrades the performance of the mesoscale model, particularly the near-surface air temperature. The two most common approaches to this problem are use of an 'offline' model, usually known as a land data assimilation system (LDAS), or an 'online' system such as an indirect nudging scheme. A third approach is variational assimilation of 2-m observations to produce soil moisture analyses. Techniques for direct assimilation of surface solar radiation estimates such as are derived from Geostationary Operational Environmental Satellite imagery show to improve this problem greatly.

## 10 SIMPLIFIED BIOSPHERE MODEL (SiB)

### 10.1 MODEL OVERVIEW

In the existing GCMs during the 1980s, the fluxes of radiation, heat (sensible and latent) and momentum across the lower boundary of the atmosphere were treated as independent processes. The surface fluxes were made to depend on an independently specified surface albedo, surface roughness length or drag coefficient and formulated dependence of evapotranspiration on soil moisture. The land surface properties might be independently prescribed as boundary conditions within the GCMs (General circulation models). At the same time, the land surface models took the surface boundary conditions from the GCMs.

That was the case of the hydrology model used in the National Meteorological Center (NMC) spectral GCM, which consisted of a conceptual bucket for each land point, filled by precipitation and emptied by evaporation and runoff. This scheme cannot be considered as a realistic description of the energy partition process as it actually occurs in nature (Sato et al., 1989). The most important omission of the bucket model was that of biophysical control of transpiration: vegetation can exert a considerable resistance on the transfer of water from soil to atmosphere and this can reduce the evapotranspiration rate to a level significantly below that calculated with the bucket formulation.

But since then, the scientific community recognized the need of modeling the two-way interaction between the atmospheric models and the land surface models. One of the earliest models that was proposed to describe the Biosphere, suitable for operation within (CGMs) was the Simple Biosphere Model (SiB), first developed by (Sellers et al., 1986). The model was intended to be as physically and biologically realistic as possible to provide the fluxes of sensible and latent heat, and momentum, than the existing formulations at the moment.

The Simple Biosphere model (SiB) of (Sellers et al., 1986) models the vegetation itself and let the vegetation determine the ways in which the land surface interacts with the atmosphere, since plants are alive. It directly addresses the effect of vegetation on land surface-atmosphere interactions by modeling those physiological and biophysical processes which influence radiation, momentum, mass and heat transfer.

### 10.2 MODEL STRUCTURE

The morphological and physiological characteristics of the vegetation community in a grid area are used to derive coefficients and resistances that govern the momentum, radiation and heat fluxes between the surface and the atmosphere. All of these fluxes depend upon the state of the vegetated surface and the atmospheric boundary conditions, which are defined below.

### 10.2.1 ATMOSPHERIC BOUNDARY CONDITIONS

The upper boundary conditions for SiB are given by the following parameters:

- Air temperature, vapor pressure and wind speed of the lowest model layer
- The solar zenith angle
- Five components of the incident radiation
- Large scale and convective precipitation rates

### 10.2.2 MORPHOLOGICAL PARAMETERS

In SiB, the world's vegetation is classified into twelve types of biomes. It is also divided into two morphological groups: trees or shrubs, which constitute the upper story or canopy vegetation, and the ground cover, which consists of grasses and other herbaceous plants. Either, both or neither of these vegetation covers may be present in a given grid area (Figure 18).

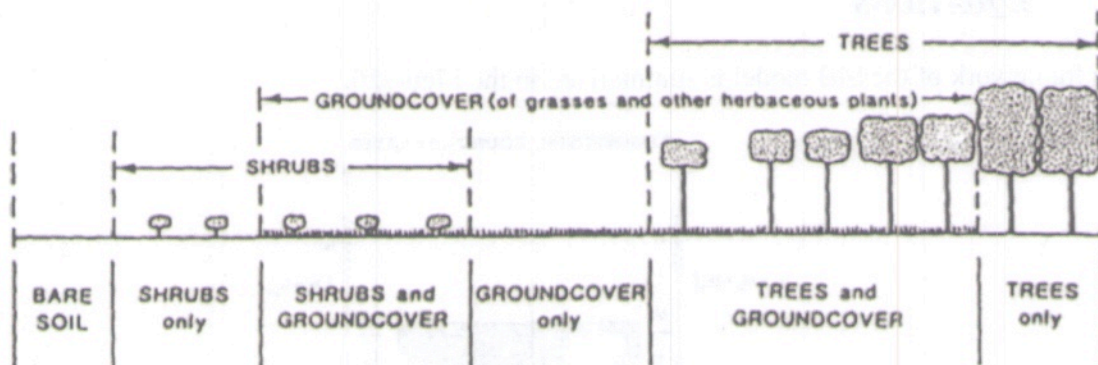


Figure 18 Vegetation morphology as represented in the Simple Biosphere Model (SiB)

The upper story vegetation consists of perennial plants with persistent roots assigned to a fixed depth taken to be the bottom of the second soil layer (Figure 19). The ground cover is made up of annual plants and may have a time-varying root depth. There is an upper, thin soil layer (soil layer 1) from which there can be a significant rate of withdrawal of water by direct evaporation into the air when the pores of the soil are at or near saturation. The root zone layer (soil layer 2) contains all the roots for the two vegetation layers. Beneath the root zone, there is an underlying recharge layer (soil layer 3) where the transfer of water is governed only by gravitational drainage and hydraulic diffusion. A three layer isothermal model is used to determine the hydraulic diffusion and gravitational drainage of water in the soil. Soil properties are assigned to each vegetation type in much the same way as the time-invariant vegetation properties. Soil-layer depths are defined as a function of vegetation type.

The snow model is very simple compared to the sophisticated vegetation and soil models. The snow depth is explicitly predicted though it is very crude. There is no explicit

treatment of snow temperature; rather, it is included in ground surface temperature for a combination of three surface types: ground vegetation, soil and snow.

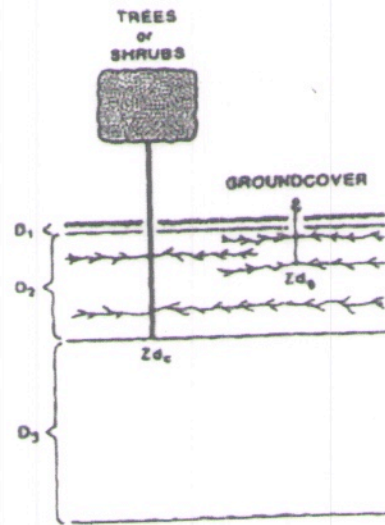


Figure 19 Root systems and soil layer of the Simple Biosphere Model (SiB)

### 10.2.3 PRONOSTIC PHYSICAL STATE VARIABLES AND THEIR GOVERNING EQUATIONS

The framework of the SiB model is summarized in the Figure20.

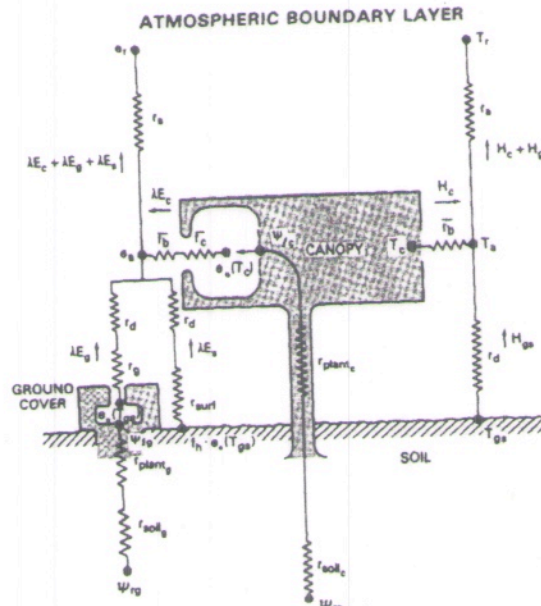


Figure 20 Framework of the Simple Biosphere Model (SiB)

The transfer pathways for latent and sensible heat flux are shown on the left and right-hand sides of the diagram, respectively. The treatment of radiation and intercepted water has been omitted for clarity.

The SiB model has eight prognostic physical-state variables:

- Three temperatures (one for the canopy vegetation, another for both the ground cover and the soil surface, and a deep soil temperature).
- Two interception water stores (one for the canopy and one for the ground cover).
- Three soil moisture stores.

The governing equations for the temperatures are given in (Sellers et al.,1986).

### **10.3 IMPROVEMENTS IN THE SiB MODEL**

The principles of the SiB model have been described above (Sellers et al.,1986) and (Sato et al.,1989). But it has since undergone several revisions. It was first extended in the mid-1990s by a team of interdisciplinary scientists to include mechanistic linkages to photosynthesis, stomatal physiology, and satellite remote sensing. It was later extended to include improved treatment of carbon cycling, soils, snow, hydrology, stable isotopes, phenology, and crops.

The first one review had the aim to simplify the model (Xue et al.,1991). The new version was named the SSiB (also called SiB2 and SSiB2) model. The most significant terms and variables in the model whose variations can affect the structure of the atmospheric boundary layer were identified. In so doing, the number of free parameters in the SiB model was reduced by a factor of two. And, while there were still 21 parameters in the reduced set (54 in the former set), many of these cannot be varied independently if a realistic parameter set is to be retained. As a result, the model was more suitable for general circulation sensitivity studies, given the more manageable size of the parameter set.

In the diurnal cycle of surface albedo computation, a complicated calculation was replaced by a harmonic fit. The major reduction of parameters was affected by simplifying the soil moisture effect on stomatal resistance as well as an elimination of two story vegetation. In the remaining 21 parameters, 14 are from vegetation. Some equations were developed to relate the Richardson number to the aerodynamic resistance and simplify the calculation, reducing the computational cost by about 55 %.

Later on, besides the reduction to a single layer of vegetation, there was a reduction in the number of vegetation classes from 12 to 9. In SiB1 (Sellers et al.,1986) soil properties were assigned to each vegetation type in much the same way as the time-invariant vegetation properties. However, soil properties exhibit regional variations that can be independent of vegetation type, and vice versa. In SiB2 (Sellers et al.,1996b), the Food Agriculture Organization (FAO) global soil-type map was combined with a table of soil properties to produce global fields of the soil physical properties. There was also an incorporation of a much simpler soil moisture stress model (Sellers et al.,1996b). The hydrological submodel was modified to give better descriptions of base flows and a more reliable calculation of interlayer exchanges within the soil profile. There was also introduced a more realistic and

universal formulation to describe canopy conductance and photosynthesis, in order to describe the simultaneous transfer of  $\text{CO}_2$  and water vapor into and out of the vegetation, respectively. Photosynthesis was not calculated in SiB1 at all. In SiB1, the parameterization of photosynthetic carbon assimilation is based on enzyme kinetics originally developed by (Farquhar et al., 1980), and is linked to stomatal conductance and hence to the surface energy budget and atmospheric climate (Sellers et al., 1996a). The phenologically varying vegetation properties were prescribed by vegetation type and month (seasonal and latitude variations). In SiB2 (Sellers et al., 1996b) all of the time and space variations related to phenological vegetation properties were calculated from the satellite data-set (Sellers et al., 1996a). There was also incorporated a "patchy" snow melt treatment, which prevents rapid thermal and surface reflectance transitions when the area-averaged snow cover is low and decreasing.

The model has been updated to include prognostic calculation of temperature, moisture, and trace gases in the canopy air space. Direct-beam and diffuse solar radiation are treated separately for calculations of photosynthesis and transpiration of sunlit and shaded canopy fractions. Other recent improvements include biogeochemical fractionation and recycling of stable carbon isotopes, improved treatment of soil hydrology and thermodynamics, and the introduction of a multilayer snow model based on the Community Land Model (Dai et al., 2003), a prognostic phenology algorithm that assimilates vegetation imagery (Stockli et al., 2008), the biogeochemical cycling of carbon among decomposing organic pools (Schaefer et al., 2008), and the ecophysiology of corn, soy, and wheat crops (Lokupitiya et al., 2008). The model was then referred to as SiB3 (also named SSiB3). The complexity of the SiB3 model is shown in the Figure 21.

The SiB1 model could be considered to belong to the "second-generation" group in the Land Surface model evolution classification (see Section 3). However, after all the improvements added in the SiB2 and SiB3 it can be considered as a "third-generation" model.

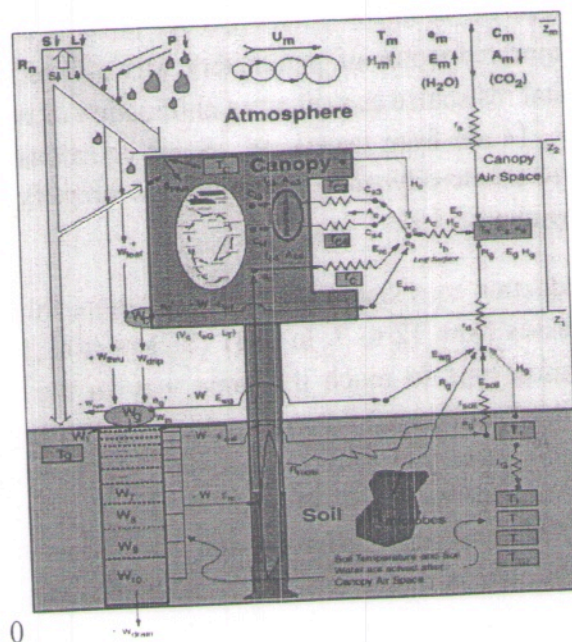


Figure 21 Framework of the modified Simple Biosphere Model (SiB3)



## 11 COMMUNITY LAND MODEL (CLM)

### 11.1 MODEL HISTORY AND OVERVIEW

The early development of the Community Land Model can be described as the merging of a community-developed land model focusing on biogeophysics and a concurrent effort at NCAR to expand the NCAR Land Surface Model (NCAR LSM, Bonan, 1996), used in the Community Climate Model CCM3 and the initial version of the Community Climate System Model (CCSM). The concept of a community-developed land component was initially proposed at the CCSM Land Model Working Group (LMWG) meeting in February 1996 and finally designated as the Common Land Model (CLM) in 1998.

The aim was to include the carbon cycle, vegetation dynamics, and river routing in the LSM. These advancements necessitated several modifications to the Common Land Model (Oleson et al., 2010). The biome-type land cover classification scheme was replaced with a plant functional type (PFT) representation with the specification of PFTs and leaf area index (LAI) from satellite data (Bonan et al., 2002). Plant functional types (PFTs) classification is a system used by climatologists to classify plants according to their physical, phylogenetic and phenological characteristics as part of an overall effort to develop a vegetation model for use in land use studies and climate models. PFTs provide a finer level of modeling than biomes, which represent gross areas such as desert, savannah, deciduous forest. In creating a PFT model, areas as small as 1 km<sup>2</sup> are modeled by defining the predominant plant type for that area, interpreted from satellite data or other means.

This also required modifications to parameterizations for vegetation albedo and vertical burying of vegetation by snow. Changes were made to canopy scaling, leaf physiology and soil water limitations on photosynthesis to resolve deficiencies indicated by the coupling to a dynamic vegetation model. Vertical heterogeneity in soil texture was implemented to improve coupling with a dust emission model. A river routing model was incorporated to improve the fresh water balance over oceans. Numerous modest changes were made to the parameterizations to conform to the strict energy and water balance requirements of CCSM. Further substantial software development was also required to meet coding standards. The resulting model was adopted in May 2002 as the Community Land Model (CLM2.0) for use with the Community Atmosphere Model (CAM2.0, the successor to CCM3) and version 2 of the Community Climate System Model (CCSM2.0).

In 2004, a project was initiated to improve the hydrology in CLM3.0 as part of the development of CLM version 3.5. A selected set of promising approaches to alleviating the hydrologic biases in CLM3.0 were tested and implemented. These included new surface datasets based on Moderate Resolution Imaging Spectro radiometer (MODIS) products, new parameterizations for canopy integration, canopy interception, frozen soil, soil water availability, and soil evaporation, a TOPMODEL-based model for surface and subsurface runoff, a groundwater model for determining water table depth, and the introduction of a factor to simulate nitrogen limitation on plant productivity.

CLM3.5 improves representations of hydrology, evapotranspiration, and snow albedo compared to the previous version, CLM3.0 (Oleson and Coauthors, 2008). For instance, CLM3.5 allows for a flexible treatment of soil water availability, with PFT dependent values of soil moisture potential at which stomatal opening and closing occurs and a nonzero range in potential between soil water saturation and the onset of water stress. These features lead to increased simulated evapotranspiration, reducing the low evapotranspiration bias found in CLM3.0. In addition, CLM3.5 corrected a snow aging parameterization deficiency in CLM3.0, partially ameliorating the delayed snowmelt in CLM3.0 relative to observations.

The coupling of WRF3 and CLM3.5 builds on a previous software coupling (Miller and Coauthors, 2009) between WRF2 and CLM3. The top-level WRF driver structure is retained, and CLM is called as a subroutine within WRF. The PFTs were assigned to grid cells according to a fixed mapping from WRF's 24 U.S. Geological Survey (USGS) land-use categories to groups of up to 4 of CLM's 17 PFTs, including bare ground (BG). The mapping is based on that used in LSM1 (Bonan, 1996). Monthly LAI is prescribed for each PFT and does not vary geographically. This approach makes the WRF3-CLM3.5 model easily accessible to the WRF community while sacrificing some of the more detailed surface data normally prescribed in CLM.

The motivation for the next version of the model, CLM4.0, was to (1) incorporate several recent scientific advances in the understanding and representation of land surface processes, (2) expand model capabilities, and (3) improve surface and atmospheric forcing datasets. A broad set of model improvements and additions have been provided through the CLM development community to create CLM4 (Lawrence et al., 2011):

- The model is extended with a carbon-nitrogen (CN) biogeochemical model that is prognostic with respect to vegetation, litter, and soil carbon and nitrogen states and vegetation phenology.
- An urban canyon model is added and a transient land cover and land use change (LCLUC) capability, including wood harvest, is introduced, enabling study of historic and future LCLUC on energy, water, momentum, carbon, and nitrogen fluxes.
- The hydrology scheme is modified with a revised numerical solution of the Richards equation and a revised ground evaporation parameterization that accounts for litter and within-canopy stability.
- The new snow model incorporates the Snow and Ice Aerosol Radiation model (SNICAR) - which includes aerosol deposition, grain-size dependent snow aging, and vertically-resolved snowpack heating- as well as new snow cover and snow burial fraction parameterizations.
- The thermal and hydrologic properties of organic soil are accounted for and the ground column is extended to 50-m depth.

- Several other minor modifications to the land surface types dataset, grass and crop optical properties, surface layer thickness, roughness length and displacement height, and the disposition of snow-capped runoff are also incorporated.

The new model exhibits higher snow cover, cooler soil temperatures in organic-rich soils, greater global river discharge, and lower albedos over forests and grasslands, all of which are improvements compared to CLM3.5. When CLM4 is run with carbon-nitrogen (CN), the mean biogeophysical simulation is degraded because the vegetation structure is prognostic rather than prescribed, though running in this mode also allows more complex terrestrial interactions with climate and climate change.

## 11.2 MAIN CHARACTERISTICS OF THE CLM4 LSM

### 11.2.1 SURFACE HETEROGENEITY AND DATA STRUCTURE

Spatial land surface heterogeneity in CLM is represented as a nested subgrid hierarchy in which grid cells are composed of multiple landunits, snow/soil columns, and PFTs (Figure 22). Each grid cell can have a different number of landunits, each landunit can have a different number of columns, and each column can have multiple PFTs.

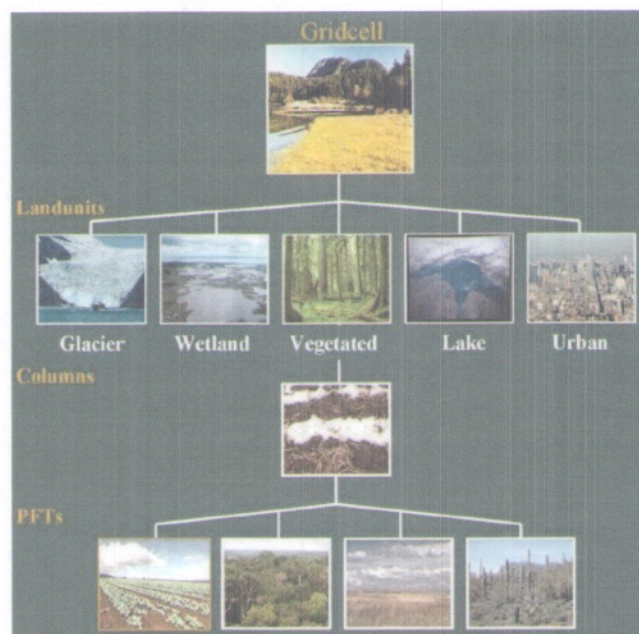


Figure 22 Current default configuration of the CLM subgrid hierarchy emphasizing the vegetated landunit. Only four PFTs are shown associated with the single column beneath the vegetated landunit but up to sixteen are possible

CLM represents the surface by five primary subgrid land units (land-cover types): glacier, lake, wetland, urban, and vegetated in each grid cell (Figure 22). The vegetated portion of a grid cell is further divided into patches of up to 4 of 16 PFTs (Bonan et al., 2002), each characterized by distinct physiological parameters (Oleson and Coauthors, 2004). Once calculations are performed at the PFT level, energy, water, and momentum fluxes are

aggregated to the gridcell level and passed to the atmospheric model. The extensive mechanistic detail and evaluation history of CLM (Bonan et al., 2002, Oleson and Coauthors, 2004, etc.) are advantageous for modeling the climate impacts of land-cover change.

The first subgrid level, the landunit, is intended to capture the broadest spatial patterns of subgrid heterogeneity. The second subgrid level, the column, is intended to capture potential variability in the soil and snow state variables within a single landunit (Figure 23). For example, the vegetated landunit could contain several columns with independently evolving vertical profiles of soil water and temperature. The central characteristic of the column subgrid level is that this is where the state variables for water and energy in the soil and snow are defined, as well as the fluxes of these components within the soil and snow. Regardless of the number and type of PFTs occupying space on the column, the column physics operates with a single set of upper boundary fluxes, as well as a single set of transpiration fluxes from multiple soil levels. These boundary fluxes are weighted averages over all PFTs in the column. Normally, for glacier, lake, wetland, and vegetated landunits, a single column is assigned to each landunit. The urban landunit has five columns (roof, sunlit and shaded wall, and pervious and impervious canyon floor (Oleson et al. 2010).

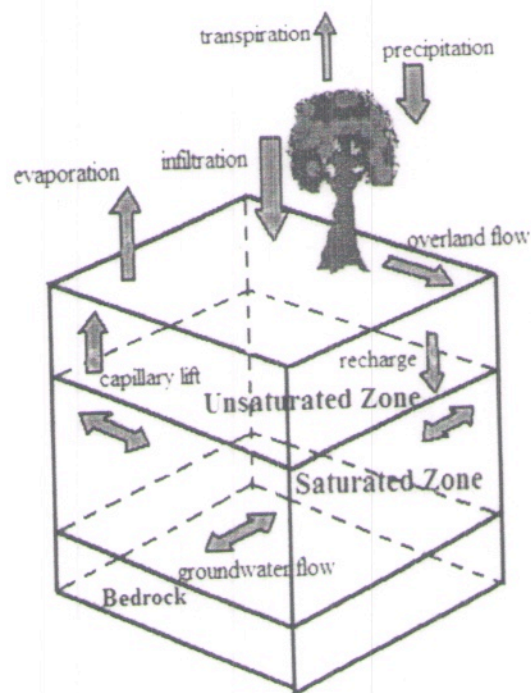


Figure 23 Typical one dimensional Soil Column in LSM Coupled with Multiple Land Surface Hydrologic Processes

The third subgrid level is referred to as the PFT level, but it also includes the treatment for bare ground. It is intended to capture the biogeophysical and biogeochemical differences between broad categories of plants in terms of their functional characteristics. All fluxes to and from the surface as the vegetation state variables (e.g. vegetation temperature and canopy water storage) are defined at the PFT level. Up to 16 possible PFTs that differ in physiology and structure may coexist in a single column:

- needleleaf\_evergreen\_temperate\_tree
- needleleaf\_evergreen\_boreal\_tree
- needleleaf\_deciduous\_boreal\_tree
- broadleaf\_evergreen\_tropical\_tree
- broadleaf\_evergreen\_temperate\_tree
- broadleaf\_deciduous\_tropical\_tree
- broadleaf\_deciduous\_temperate\_tree
- broadleaf\_deciduous\_boreal\_tree
- broadleaf\_evergreen\_shrub
- broadleaf\_deciduous\_temperate\_shrub
- broadleaf\_deciduous\_boreal\_shrub
- c3\_arctic\_grass
- c3\_non-arctic\_grass
- c4\_grass
- corn
- wheat

These 16 PFTs are adjusted to the 24 U.S.G.S. classification or any other land use classification, depending on the data source (e.g. MODIS, CORINE,etc.). The two last PFTs can be other type of crops.

Vegetation structure is defined by leaf (LAI) and stems (SAI)<sup>5</sup> area indices and canopy top and bottom heights. Separate leaf and stem area indices and canopy heights are prescribed for each PFT. Daily leaf and stem area indices are obtained from gridded datasets (1km MODIS derived) of monthly values. Canopy top and bottom heights are also obtained from gridded datasets. However, these are currently invariant in space and time and were obtained from PFT specific values (Bonan et al. 2002).

---

<sup>5</sup> SAI is the one-sided stem area per ground area, where “stem” includes dead leaves, branches, and stems.

### **11.2.2 BIOGEOPHYSICAL PROCESSES**

Biogeophysical processes are simulated for each subgrid landunit, column, and PFT independently and each subgrid unit maintains its own prognostic variables. The same atmospheric forcing is used to force all subgrid units within a grid cell. The surface variables and fluxes required by the atmosphere are obtained by averaging the subgrid quantities weighted by their fractional areas.

The processes simulated are shown in Figure 24 and include:

- Vegetation composition, structure, and phenology
- Absorption, reflection, and transmittance of solar radiation
- Absorption and emission of longwave radiation
- Momentum, sensible heat (ground and canopy), and latent heat (ground evaporation, canopy evaporation, transpiration) fluxes
- Heat transfer in soil and snow including phase change
- Canopy hydrology (interception, throughfall, and drip)
- Snow hydrology (snow accumulation and melt, compaction, water transfer between snow layers)
- Soil hydrology (surface runoff, infiltration, redistribution of water within the column, sub-surface drainage, groundwater)
- Stomatal physiology and photosynthesis
- Lake temperatures and fluxes
- Dust deposition and fluxes
- Routing of runoff from rivers to ocean
- Volatile organic compounds
- Urban energy balance and climate
- Carbon-nitrogen cycling
- Dynamic landcover change
- Dynamic global vegetation

### 11.2.3 SHEMES AND ASSUMPTIONS IN CLM

Some of the most important assumptions and schemes used in the CLM LSM are:

- CLM includes a 5-layer snow scheme, a 10-layer soil scheme, and a single-layer vegetation scheme with a sunlit and shaded canopy (Dai et al., 2003) and (Oleson and Coauthors, 2004).
- The two-stream approximation (Sellers, 1992) is applied to calculate solar radiation reflected and absorbed by the canopy as well as its transfer within the canopy.
- Temperature and humidity are allowed to be different at the ground surface, in the canopy, and at the leaf surface.
- Stomatal conductance is based on a mechanistic prediction of photosynthesis and its relationship to environmental conditions.
- CLM partitions evapotranspiration into transpiration, soil evaporation, and canopy evaporation (Lawrence et al., 2007).
- Solid ice, liquid water, and temperature are prognostic variables for each snow layer, and the snow density and albedo are adjusted as the snow undergoes aging and compaction. The snow albedo calculation over vegetation cover also includes a calculation of fractional snow cover based on the snow height.

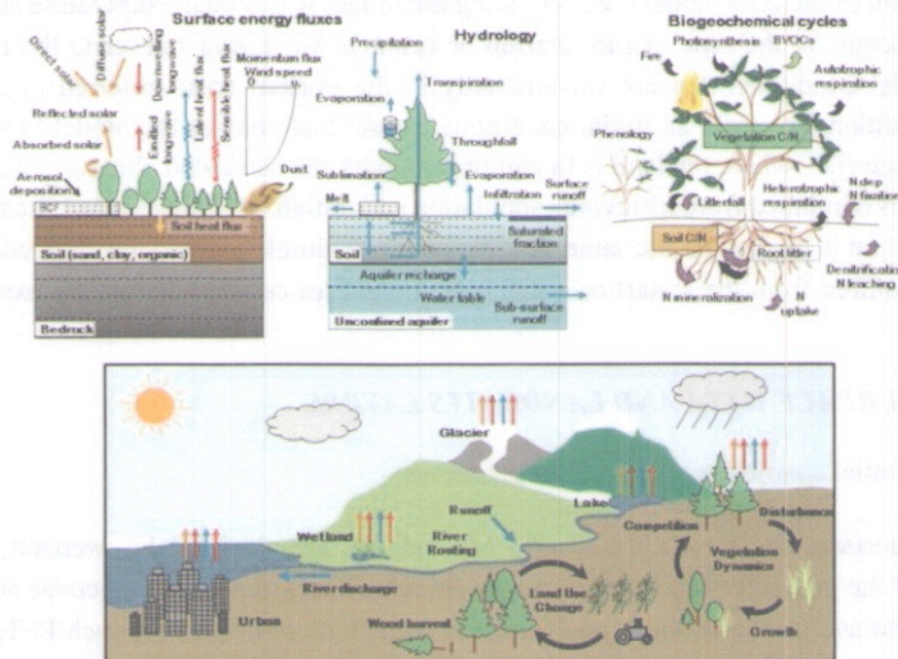


Figure 24 Biogeophysical processes in CLM4 (from Lawrence et al, 2010)

## **11.3 MODEL REQUIREMENTS**

### **11.3.1 ATMOSPHERIC COUPLING**

The current state of the atmosphere -including variables as wind, potential temperature, humidity, incident radiation, carbon dioxide concentration, aerosol and nitrogen deposition rate- at a given time step is used to force the land model. This atmospheric state is provided by an atmospheric model in coupled mode. The land model then initiates a full set of calculations for surface energy, constituent, momentum, and radiative fluxes (Oleson et al, 2010).

The land model calculations are implemented in two steps: First, it proceeds with the calculation of surface energy, constituent, momentum, and radiative fluxes using the snow and soil hydrologic states from the previous time step. Then, it updates the soil and snow hydrology calculations based on these fluxes. These fields are passed to the atmosphere. The land model output to the atmospheric model includes variables as latent and sensible heat fluxes, water vapor flux, momentum flux, emitted radiation, albedo, absorbed solar radiation, radiative temperature, temperature and specific humidity at 2m height, snow water equivalent, aerodynamic resistance, friction velocity, dust flux and net ecosystem exchange. The albedos sent to the atmosphere are for the solar zenith angle at the next time step but with surface conditions from the current time step.

### **11.3.2 INITIALIZATION**

Initialization of the land model (i.e., providing the model with initial temperature and moisture states) depends on the type of run (startup or restart). An startup run starts the model from either initial conditions that are set internally in the Fortran code (referred to as arbitrary initial conditions) or from an initial conditions dataset that enables the model to start from a spun up state (i.e., where the land is in equilibrium with the simulated climate). In restart runs, the model is continued from a previous simulation and initialized from a restart file that ensures that the output is bit-for-bit the same as if the previous simulation had not stopped. The fields that are required from the restart or initial conditions files can be obtained by examining the code.

### **11.3.3 SURFACE DATA AND LANDUNITS LAYERS**

Arbitrary initial conditions are specified as follows:

Required surface data for each land grid cell include: the glacier, lake, wetland, and urban portions of the grid cell (vegetation occupies the remainder); the fractional cover of each PFT; monthly leaf and stem area index and canopy top and bottom heights for each PFT; soil color; soil texture, and soil organic matter density. A number of urban parameter fields are also required.



Soil color determines dry and saturated soil albedo. The sand, clay, and organic matter content determine soil thermal and hydrologic properties. The maximum fractional saturated area is used in determining surface runoff and infiltration.

Vegetated, wetland, and glacier landunits have fifteen vertical layers, whereas lakes have ten. For soil points, temperature calculations are done over all layers,  $N_{levgrnd} = 15$ , whereas hydrology calculations are done over the top ten layers,  $N_{levsoi} = 10$ , the bottom five layers being specified as bedrock.

## 12 LAND SURFACE MODELS COMPARISON

In this document, the most important characteristics of seven land surface models (LSMs) have been analyzed: the 5-Layer Thermal diffusion (5-Layer), Noah (Noah), Noah with Multi-parameterizations (Noah-MP), Rapid Update Cycle (RUC), Pleim and Xiu (PX), Simplified Biosphere (SSiB) and Community Land Model (CLM).

The text is focused on understanding the characteristics of the different LSMs, in order to facilitate the interpretation of the behaviour of the WRF model in experiments in which different configurations can be used to simulate the surface wind field. So, in this section the comparison of the LSMs based on their main characteristics gathered from the literature will be addressed.

### 12.1 SOIL LAYERS

The number and depth of the soil layers in a surface model is a key factor, not only because the complexity of the processes requires taking into account deep soil layers but also because the long term processes need for a soil depth enough to study climate anomalies. Shallow columns are not able to capture the critical zone (down to 5 m) to which the surface energy budgets are most sensitive.

The 5-Layer model includes 5 thin layers, with a maximum depth of 63 cm (Table 1). The PX model includes only 2 layers with a total depth of 1m. These two models are, therefore, incapable of including important processes that need for deep soil interaction. The SSiB model includes three layers, corresponding to the surface, root and recharge zones with variable thickness, depending on the vegetation type. Noah includes four soil layers, with a total depth of two meters and a 1-m thick aquifer, whereas Noah-MP had, at the beginning, the same four layers plus an unconfined aquifer added at the bottom, but there are currently many options with a variable number of layers, with a maximum depth of 8m. RUC has either 6 or 9 (last version) prognostic levels, with a total depth of 3m, and CLM includes 15 layers for soil temperature calculations and 10 layers for hydrology calculations, with a total depth between 50m and 150m (up to 50 m in practice).

Therefore, regarding the soil layers' depth and distribution, both the Noah-MP and CLM models are much more advantageous than the other ones, because they can address climate processes that need for deep soil layers accounting. Nevertheless, the CLM model seems to be the best one in this matter, since it considers much more layers and higher total depth, which allows for better soil influence on the surface processes.

	No. OF SOIL LAYERS	SOIL LAYERS DEPTH (cm)	MAXIMUM SOIL LAYERS DEPTH (m)
<b>5-Layer</b>	5	1, 2, 4, 8, 16	0.63
<b>Noah</b>	4	10, 30, 60 (root zone) 100 (reservoir)	2
<b>Noah-MP</b>	4 (variable) +unconfined aquifer	10, 30, 60 (root zone) 100 (reservoir) variable	up to 8
<b>RUC</b>	6 (past) 9 (now)	0,5,20,40,160,30 0,1,4,10,30,60,100,160,300	3
<b>PX</b>	2	1(surface layer), 100 (reservoir)	1
<b>SSiB</b>	3	depending on vegetation type surface, root, recharge	variable
<b>CLM</b>	15 for temperature 10 for hydrology	variable	up to 50-150 m

Table 1 Soil layers characteristics in the 5-Layer, Noah, Noah-MP, RUC, Pleim and Xiu (PX), SSiB and CLM and models

## 12.2 LAND USE AND SOIL TEXTURE

The 5-Layer, SSiB, Noah and Noah-MP do not have sub-grid cells within its model grid cell, but the Noah and Noah-MP include a subtiling option, allowing for canopy gaps, in the MP case (table 2). The PX model allows for fractional coverage for land use and soil, whereas the RUC model allows for subgrid heterogeneity and seasonal variations. The CLM allows for 10 subgrid levels per grid cell to better represent subgrid heterogeneity of the land surface. Thus, it is this last LSM (CLM) the one seems to include a better representation of the land surface heterogeneity in a grid cell.

The Noah model used to take the vegetation type from the 1km resolution 24 U.S.G.S. land use data, that are also used in the RUC model (as default) and the PX model, although it now uses the 20-category land use classification derived from the Moderate Resolution Imaging Spectroradiometer (MODIS) satellite observations, as it is used in the Noah-MP model and, as an option, in the RUC model. In the SiB1 model there used to be 12 biome type land use categories (that give better information from the biological point of view than the USGS) but they were reduced to 9 in the SSiB2 and SSiB3. The 24 United States Geological Survey (USGS) land use types are translated to the 16 plant functional types (PFTs) in CLM based on a lookup table. The PFTs are considered to better represent the vegetation classification than the biome types. But in CLM, spatial land surface heterogeneity is represented as a nested subgrid hierarchy in which grid cells are composed of multiple landunits, snow/soil columns, and PFTs, so that the complexity and characterization of the land surface goes beyond the other models' limits.

	SOIL TEXTURE	LAND USE CATEGORIES	No. OF VEG.TYPE/CELL	URBAN PHYSICS
5-Layer	16	16	1	no
Noah	16 up to 19	16 (early version) 24 U.S.G.S(past) 20 MODIS (now)	1 subtiling option	no
Noah-MP	19	20 MODIS	Semi-tile, allowing for canopy gaps	yes
RUC	19	24 U.S.G.S.(default) 20 MODIS (option)	Subgrid heterogeneity Seasonal variations	no
PX	11 (USDA)	24 U.S.G.S.	Fractional coverage for land use and soil	no
SSiB	-16 fixed (SiB1) - Time-variable (SSiB2-3) from FAO soil-type map	- 12 biomes(SiB1) - 9 biomes (SSiB2,SSiB3)	1	no
CLM	- 19 categories percentage of sand and clay - Vertical heterogeneity	- 5 land units - Different columns - 4-16 PFT'S assigned to 24 U.S.G.S classes	10 subgrid levels/grid	yes

Table 2 Land-use and soil texture categories in the 5-Layer, Noah, Noah-MP, RUC, Pleim and Xiu (PX), SSiB and CLM and models

In order to characterize the soil texture, it is divided into categories defined as percentages of sand and clay. In the case of the Noah there used to be 16 categories but there are 19 in recent versions, as well as in the Noah-MP, RUC and CLM models. The PX soil texture is based on the USDA 11 categories classification. SiB1 included 16 fixed categories, SSiB includes a time-variable classification based on the FAO soil-type map. CLM also considers vertical heterogeneity in the column. The only models that include urban physics are the Noah-MP and the CLM models.

It can be concluded that the most complete land use and soil texture classification is the one used in the CLM model, followed by the Noah-MP.

### 12.3 CANOPY STRUCTURE, VEGETATION SCHEME AND DATA ASSIMILATION

The 5-Layer model does not include any canopy interaction (table 3). In Noah, there was a combined surface layer vegetation-soil (only separated in the improvements added while the transition to Noah-MP) and the heat and water fluxes between the bottom of the canopy and the soil/snow surface are not described. In Noah-MP there is a separated vegetation canopy layer and it could be coupled with a dynamic vegetation 3D model and distinguish between canopy top and bottom. In RUC vegetation is also separated from soil and is accounted for the hydrology aspects. CLM, PX, and SSiB models have a single-layer vegetation scheme, with sunlit and shaded canopy, although SiB1 used to have 2 canopy layers.

	CANOPY STRUCTURE	VEGETATION SCHEME	No. OF CANOPY LAYERS	DATA ASSIMILATION
<b>5-Layer</b>	- No canopy interaction	no	0	no
<b>Noah</b>	- Combined surface veg-soil - No fluxes canopy-soil	- Pan and Mahrt scheme	1	- Past: AVHRR (0.15) radiometer data - Present: MODIS satellite data
<b>Noah-MP</b>	- 3-D structure - Vegetation separated from soil	- Pan and Mahrt scheme - Photosynthetically active radiation (PAR) model - Two-stream canopy radiation transfer - Dynamic veg. model	Canopy top and bottom	- Past: AVHRR (0.15) radiometer data - Present: MODIS satellite data
<b>RUC</b>	- Vegetation separated from soil	- Pan and Mahrt scheme - Aerodynamic roughness length, LAI and emissivity	1	- Past: AVHRR (0.30) radiometer data - Present: MODIS satellite data
<b>PX</b>	- Canopy shelter factor	- Land-use derived parameters - ISBA model for vegetation interaction	1	- LDAS (land data assimilation system) - Nudging scheme Satellite data
<b>SSiB</b>	- Sunlit and shadow	- Phenologically varying model - 12 (SiB1) or 9 (SiB2-3) types of biomes - 2 morphological groups - Dynamic model: - Land cover change - Global vegetation	2 (SiB1) 1 (SSiB2, SSiB3)	- Satellite data
<b>CLM</b>	- Single-layer scheme for sunlit and shaded canopy	- Stomatal physiology - Photosynthesis - Carbon-nitrogen biogeochemical forecasting model	1	- Snow Telemetry (SNOTEL) - MODIS Satellite data

Table 3 Canopy structure, vegetation scheme and data assimilation in the 5-Layer, Noah, Noah-MP, RUC, Pleim and Xiu (PX), SSiB and CLM and models

The vegetation scheme in the Noah, Noah-MP and RUC models is taken from that in (Pan and Mahrt,1987). In the case of Noah-MP, a photosynthetically active radiation model (FPAR), a dynamical vegetation model and a two-stream canopy radiation transfer are added. The RUC model uses aerodynamic roughness length, LAI and emissivity. The PX uses the ISBA model for vegetation interaction, the SSiB model uses a phenologically varying model. The two-stream approximation (Dickinson et al.,1987) is applied to the vegetation to calculate solar radiation reflected and absorbed by the canopy as well as its transfer within the canopy, in the CLM model. But the most important improvement in CLM is the use of a dynamic vegetation model (like in the Noah-MP). It includes land cover change, global vegetation, stomatal physiology, photosynthesis and a carbon-nitrogen biogeochemical forecasting model.

The Noah, Noah-MP and RUC models used to assimilate data from the AVHRR radiometer, changing later to the MODIS satellite data (table3). The PX model uses the land data assimilation system (LDAS). CLM also uses MODIS satellite data, joined to the automated Snow Telemetry (SNOTEL) station data over the Columbia River Basin in the northwestern United States are used to evaluate snowmelt simulations generated with the coupled WRF-CLM model.

It is difficult to compare the vegetation scheme of the different LSMs, because most of them have added important improvements lately, but, once again, it could be said that both CLM and Noah-MP models stand out from the other models, especially because of the integration of a Dynamic vegetation model, which allows for simulating future climate-forced vegetation shifts.

## 12.4 HYDROLOGY

Although the seven models differ in many aspects, one of the main differences among them lays on the treatment of the soil moisture and hydrology (table 4). They differ both in the number of processes taken into account to calculate the soil moisture and water, and in the complexity of the schemes used for this calculations.

In the 5-Layer model the soil moisture content is fixed to climatological values, that just depend on the land use category of each grid cell, and does not change throughout the entire simulated period (only distinguish values between winter and summer). Conversely, in the other LSMs different schemes are used for soil moisture diffusivity, hydraulic conductivity, canopy interception, superficial runoff and drainage.

The Noah, Noah-MP and RUC models use the Richard's equation to calculate the soil moisture diffusivity whereas CLM uses a modified version of this equation, the PX model uses the ISBA (Interaction Soil Biosphere Atmosphere) model, and the SSiB model uses a three-layer isothermal model. SSiB includes 3 layers for isothermal hydraulic diffusion.

The hydraulic conductivity is treated as a function of soil water content for both the Noah and the Noah-MP models, and the moisture stress factor is a function of soil moisture for both of them, but in the Noah-MP there are added two options (matric potentials functions of soil types), that are included in CLM as well. SSiB includes a soil moisture stress model.

	SOIL MOISTURE AND HYDROLOGY SCHEMES	EVAPORATION-TRANSPIRATION	RUNOFF
<b>5-Layer</b>	<ul style="list-style-type: none"> <li>- No soil moisture prediction no time variations (variables for winter and summer)</li> <li>- depending only on land use category</li> </ul>	<ul style="list-style-type: none"> <li>- Soil evaporation</li> <li>- No canopy transpiration</li> </ul>	No runoff treatment
<b>Noah</b>	<ul style="list-style-type: none"> <li>- Richard's equation for soil moisture diffusivity</li> <li>- Hydraulic conductivity function of soil water content</li> <li>- Moisture stress factor as a function of soil moisture</li> </ul>	<ul style="list-style-type: none"> <li>- Soil evaporation</li> <li>- Canopy evaporation (Diurnal Penman approach)</li> <li>- Canopy transpiration (Ball-berry equation)</li> </ul>	Simple Water Balance Model (SWB)
<b>Noah-MP</b>	<ul style="list-style-type: none"> <li>- Richard's equation for soil moisture diffusivity</li> <li>- Hydraulic conductivity function of soil water content</li> <li>- Moisture stress factor as a function of soil moisture</li> <li>+ two options (matric potentials function of soil types)</li> </ul>	<ul style="list-style-type: none"> <li>- Soil evaporation</li> <li>- Canopy evaporation (Diurnal Penman approach)</li> <li>- Canopy transpiration (Ball-berry equation)</li> <li>+Jarvis type stomatal resistance</li> </ul>	Simple Water Balance Model (SWB) + TOPMODEL
<b>RUC</b>	<ul style="list-style-type: none"> <li>- Richard's equation for soil moisture diffusivity</li> <li>- Include phase changes</li> <li>- Include gravitational motion</li> </ul>	<ul style="list-style-type: none"> <li>- Soil evaporation</li> <li>- Canopy evaporation</li> <li>- Canopy transpiration</li> </ul>	Include runoff from melting of snow water
<b>PX</b>	<ul style="list-style-type: none"> <li>- Soil moisture and evaporation (ISBA model)</li> <li>- Dynamic C10adjustment of soil moisture water intercepted by canopy</li> </ul>	<ul style="list-style-type: none"> <li>- Soil evaporation (depending on atmospheric variables)</li> <li>- Canopy evaporation (dep. on atmospheric variables)</li> <li>- Canopy transpiration(dep. on atmospheric variables)</li> </ul>	Superficial runoff surface drainage
<b>SSIB</b>	<ul style="list-style-type: none"> <li>- 3 layers isothermal hydraulic diffusion</li> <li>- 3 layers isothermal gravitational drainage</li> <li>- soil moisture stress model</li> </ul>	<ul style="list-style-type: none"> <li>- Soil evaporation (controlled by physics)</li> <li>- Canopy evaporation (controlled by physics)</li> <li>- Canopy transpiration</li> </ul>	Drainage in the third deepest layer
<b>CLM</b>	<ul style="list-style-type: none"> <li>- Modified Richard's equation for soil moisture diffusivity</li> <li>- River routing model</li> <li>- Groundwater discharge and recharge to simulate changes in canopy water</li> <li>- Matric potentials function of soil types and water</li> </ul>	<ul style="list-style-type: none"> <li>- Soil evaporation (two-stream approximation)</li> <li>- Canopy evaporation (two-stream approximation)</li> <li>- Canopy transpiration</li> <li>- Water canopy interception and drip</li> </ul>	TOPMODEL for surface and sub-surface runoff Groundwater model for water table depth Drainage of water in the unconfined aquifer

Table 4 Hydrology, soil moisture, groundwater interaction and related runoff production in the 5-Layer, Noah, Noah-MP, RUC, Pleim and Xiu (PX), SSiB and CLM and models

The PX model includes the ISBA model for soil moisture and evaporation, besides a dynamic adjustment of soil moisture water intercepted by canopy.

All the models include evaporation both from canopy and soil, and canopy transpiration (except for the 5-Layer model that doesn't include canopy effects), but they differ in the way these processes are treated. For instance, in the case of the Noah and Noah-MP models, the Diurnal Penman approach is used to calculate the canopy evaporation, also controlled by physics in the case of the SSiB model, depending on atmospheric variables in the case of PX, and using a two-stream approximation in CLM.

Regarding the canopy transpiration, it is addressed using the Ball-Berry equation (to calculate the stomatal conductance) in the case of the Noah and Noah-MP models, although in the last one there is also another option using the Jarvis type stomatal resistance. In the case of the PX model, the canopy transpiration depends on atmospheric variables. The CLM model takes into account not only the canopy evaporation and transpiration, but also the canopy drip and water interception, using more complex formulations

The runoff is not addressed in the 5-Layer model. Noah and Noah-MP use the Simple-Water Balance Model (SWB), although in Noah-MP there is another option to use the TOPMODEL for runoff calculations, that is also used in CLM. RUC and CLM include runoff from melting of snow water. PX include superficial runoff and surface drainage, whereas the SSiB model include drainage only in the third deepest layer. CLM also includes subsurface drainage and water in the unconfined aquifer, as well as the Noah-MP does (the aquifer being confined to a 1m-layer in the case of the Noah model).

## 12.5 SNOW LAYERS

The 5-Layer model does not include snow prediction at all (table 5). Noah has a single slab snow layer lumped with the soil layer, which is set to 10 cm depth, whereas in Noah-MP there are up to three layers (up to 4.5, 5 and 20 cm depth), RUC has one or two snow levels (up to 7.5 cm depth), PX has one layer, CLM has a five-layer snow scheme, with variable depth and SSiB has a multilayer based on CLM scheme, with explicit predicted depth.

Solid ice and liquid water are described in the CLM snowpack as prognostic variables. Liquid water in snow is not described in the other models, excepting the RUC, where snow physics is oversimplified -compared to CLM-, although Noah-MP includes refreezing melt-water.

In Noah there is a simple snow-ice model, with a bulk-layer snow-soil, whereas in Noah-MP there is a more permeable frozen soil, with a snow interception model, improving sublimation and albedo. In the RUC model there is a frozen soil physics algorithm and treatment for sea ice, snow melting and mixed phase. In CLM, a sophisticated snow compaction scheme is used to calculate the height and density of snow, where snow density is a critical variable for describing the water and heat transfer within the snowpack. There are also included both snow over vegetation and snowcapped runoff. Snow density and albedo are variable. The model physically describes frozen soil processes and their impact on soil properties.



	N. OF SNOW LAYERS	SNOW LAYERS DEPTH (cm)	LIQUID WATER	SNOW PHYSICS
<b>5-Layer</b>	No snow prediction	----	----	----
<b>Noah</b>	1	10	no	- Simple scheme, bulk layer snow-soil
<b>Noah-MP</b>	-Up to 3 -depending on snow depth	Variable up to 4.5, 5, 20	refreezing melt water	- Snow interception model - Improves sublimation and albedo
<b>RUC</b>	-1 or 2 -depending on snow depth	Variable up to 7.5	yes (13%)	- Frozen soil physics - Treatment for sea ice - Snow melting and mixed phase
<b>PX</b>	1	variable	no	- No accumulation, sublimation or melting of snow - It uses snow cover data from NAM-NCEP - Fractional snow coverage function of land use and snow depth
<b>SSiB</b>	-Multilayer (SSiB2-3) -Based on CLM	Explicit predicted	no	-No treatment of snow temperature - SSiB3 patchy snow melt treatment - Sea-ice treatment - Sophisticated snow compaction scheme - Variable snow density and albedo
<b>CLM</b>	5 5+5 on lake ice	Variable	yes	- Snow over vegetation - Snow capped runoff - Snow and Ice Aerosol Radiation model (SNICAR)

Table 5 Snow treatment in the 5-Layer, Noah, Noah-MP, RUC, Pleim and Xiu (PX), SSiB and CLM and models

CLM uses SNOTEL (Snow Telemetry) data, which include snow water equivalent (SWE), precipitation, and temperature. It has been proven that more realistic snow surface energy allocation in CLM is an important process that results in improved snowmelt simulations when compared to that in Noah and RUC. Additional simulations with WRF-CLM at different horizontal spatial resolutions indicate that accurate description of topography is also vital to SWE simulations.

## 13 CONCLUSIONS

Feedbacks between the land surface and atmosphere can be grouped into two categories: biogeophysical (our focus) and biogeochemical. Biogeophysical feedbacks result from energy, momentum, and moisture exchanges between the land surface and the atmosphere and are affected by soil and canopy radiative properties, surface roughness, leaf area index (LAI), stomatal resistance, rooting depth, vegetation composition and structure, among other variables. Many different processes should also be taken into account, like snow-ice treatment, hydrology, vegetation variability in space and time, lake characteristics, runoff, urban characteristics, etc.

The land surface controls the partitioning of available net radiation into sensible and latent heat fluxes. The evolution and maximum depth of the Planetary Boundary Layer (PBL) is highly dependent on this partitioning. It also controls the partitioning of available water between evaporation and runoff. Besides, the land surface is also the location of the terrestrial carbon sink.

All these processes are addressed in the Land Surface Models (LSMs) and help Atmospheric models better predict the atmosphere behaviour, since the LSM provide the initial and boundary conditions (in the surface layer) to the atmospheric models. They are critical in influencing the PBL structure, associated clouds and precipitation processes. As mesoscale models continue to increase in spatial resolution, the density of the observation network is unable to capture the initial mesoscale structure at small scales. The majority of such mesoscale structures that are missed by the observation network are, in reality, a result of land surface forcing by topography, soil moisture, surface vegetation, and soil characteristics. Therefore, it is paramount that mesoscale models include an advanced and robust Land Surface Model (LSM) in order to properly initialize the state of the ground during a data assimilation period and to subsequently capture the mesoscale structures in the free atmosphere and PBL forced by the ground surface.

This document is the result of extensive bibliographic research on Land Surface models that can optionally be used in the Weather Research and Forecasting model (WRF, Skamarock et al., 2008). The text is focused on understanding the characteristics of seven different LSMs, in order to facilitate the interpretation of the WRF model behaviour in experiments in which different configurations can be used to simulate the surface wind field. At the moment, there are not many studies addressing the influence of LSM on the wind behavior, but it is important to be analyzed, since the land surface changes modify the heat and momentum fluxes (among many other variables) that subsequently modify the low level wind, and even the upper wind, because of turbulence effects. The optional land surface schemes comparison can lead to a better understanding of how land surface processes affect regional climate and also give insight on how the land surface model complexity level affects the accuracy of regional climate simulations.

It is not easy to compare the LSMs theoretically since there is not a single criterion to ascertain which one performs best, but it depends on many factors and also depends on the LSM target. In this document, the search is focused on the possibility of reproducing the

natural processes in the land surface that affects the atmosphere -and particularly, the wind- as accurately and precisely as possible , and consuming the less time and resources as possible. But usually, the more complexity of the processes involved, the more computational time and resources required.

The seven models analyzed are the most commonly used options when running the WRF model: 5-Layer Thermal diffusion (5-Layer), Noah (Noah), Noah with Multi-parameterizations (Noah-MP), Rapid Update Cycle (RUC), Pleim and Xiu (PX), Simplified Biosphere (SSiB) and Community Land Model (CLM). The most important characteristics of these LSMs have been analyzed and compared to one another, bearing in mind that it is not easy to compare theoretical schemes without being applied to the same experimental cases.

Among the seven LSMs analyzed, RUC is the only one that is an atmospheric model itself, but since it has an important component devoted to the land surface parameterization, it can be coupled to another atmospheric model -like WRF, in this case- providing the land surface inputs for the weather modelling. RUC runs at the highest frequency of any forecast model at NCEP, assimilating recent observations to provide hourly updates of current conditions (analyses) and short-range numerical forecasts.

The number and depth of the soil layers in a surface model is crucial, not only because the complexity of the processes requires taking into account deep soil layers but also because the long term processes need for a soil depth enough to study climate anomalies. Shallow columns are not able to capture the critical zone (down to 5 m) to which the surface energy budgets are most sensitive. Among the seven LSMs analyzed, only the CLM and Noah-MP models consider a total soil depth higher than 5m. This fact makes these two models - especially CLM- more appropriate for climate considerations.

The soil texture and land use classification are also key inputs for the models. CLM allows for 10 sub-grid levels per grid cell to better represent sub-grid heterogeneity of the land surface, whereas the other models do not have sub-grid cells, although they can allow for canopy gaps (Noah-MP), fractional coverage (PX) or heterogeneity and seasonal variations (RUC). The soil texture is usually classified in 16 or 19 categories, based on the percentage of sand and clay, but the only model that includes vertical heterogeneity is CLM.

Almost all the models used to gather the land use data from the 24 U.S.G.S categories, changing to the 20 MODIS classes lately. Nevertheless, any other assimilation satellite data could be chosen as input for any of them, being translated into their own classification. In the case of the SSiB model it uses 9 biome types. But it is the CLM model which includes a more complex land surface heterogeneity, represented as a nested subgrid hierarchy in which grid cells are composed of multiple landunits, snow/soil columns, and Plant Functional Types (PFTs), so that the complexity and characterization of the land surface goes beyond the other models' limits.

Regarding the soil moisture and hydrology schemes, Noah, Noah-MP and RUC use Richard's equation for soil moisture diffusivity, which has been modified in the CLM model. The PX model instead, uses the ISBA model and there is a dynamic adjustment of soil moisture, which may make this model more appropriate for places where hydrology plays an important

role. All the models include evaporation both from canopy and soil, and canopy transpiration -except for the 5-Layer model that doesn't include canopy effects- but they differ in the way these processes are treated. CLM uses more complex schemes and takes into account changes in time, canopy drip and water interception, whereas Noah-MP have also different options - like Jarvis type stomatal resistance-.

It is difficult to compare the vegetation scheme of the different LSMs, because most of them have added important improvements lately, but only CLM and Noah-MP include a Dynamic vegetation model, which allows for simulating future climate-forced vegetation shifts, accounting for land cover, global vegetation, stomatal physiology, photosynthesis and carbon-nitrogen biogeochemical changes. Depending on the target place, it will also be important to use an LSM that includes a robust snow scheme, accounting for sublimation, mixed phase, frozen soil physics, snow melting, and even variability in snow density, as is the case of CLM. RUC and Noah-MP also include quite complete snow schemes, although they do not address snow variability.

Paying attention to the LSM evolution and classification (Section 3), it is clear that the 5-Layer thermal model cannot be compared to the rest of the models, since it does not include any vegetation interaction with the soil and atmosphere, no snow treatment and a simple soil and land use characterization, so that it is considered as a 'first generation' model. Noah combines characteristics from both 'first- and second-generation' models, whereas Noah-MP combines characteristics from both 'second- and third-generation' models, since it added new vegetation interaction and dynamic variables, among many other possibilities and parameterizations. The SiB1 model could be considered as a 'second-generation' model but, after all the improvements added in the SiB2 and SiB3, introducing important processes related to the biosphere and a phenologically varying model, it can be considered as a 'third-generation' model. Nevertheless, a priori, SSiB does not seem to be as complete as CLM or Noah-MP to be coupled to WRF in order to influence the wind behavior. The PX model can be classified as a 'second-generation' model. RUC could be considered a 'second-generation' model, but it has lately included some processes (like FPAR) more typical of the 'third-generation' models. Finally, there is no doubt that CLM is a 'third-generation' model, since it includes complex processes, involving dynamic vegetation and soil, snow treatment, etc. CLM also includes an urban model and a river routing model. Although increasing complexity does not always lead to improved model performance, it can be concluded that the CLM model is, by far, the most complex and robust LSM among the seven models analyzed in this document.

Despite the theoretical comparison, the best way to compare the LSMs should be to assess their performance in particular experiments as all the ones cited in this document. And it is most probable that there is not an absolute 'winner' that outperforms the other ones in all cases. An added obstacle to choose the best option is the fact that there are many options in each LSM, like the options in the Weather models. In any case, depending on the particular objective, it will be necessary to look for the best option based on a previous analysis of the goals to achieve, in order to fit the expectations.

## 14 REFERENCES

- [1] Anderson, J., E. Hardy, J. Roach, and R. Witmer, 1976: A land use and land cover classification system for use with remote sensor data. *U.S. Geological Survey Professional Paper*, **964**, 28.
- [2] Barnett, T., L. Dumenil, U. Schlese, E. Roeckner, and M. Latif, 1989: The effect of eurasian snowcover on regional and global climate variations. *Journal of the Atmospheric Sciences*, **46**, 661–685.
- [3] Benjamin, S., 1989: An isentropic meso-scale analysis system and its sensitivity to aircraft and surface observations. *Mon. Wea. Rev.*, **117**, 1586–1603.
- [4] Benjamin, S. and Coauthors, 2016: A north american hourly assimilation and model forecast cycle: The rapid refresh. volume 144, 1669–1694. URL <https://doi.org/10.1175/MWR-D-15-0242.1>
- [5] Benjamin, S. D. D., S. Weygandt, K. Brundage, J. Brown, G. Grell, D. Kim, B. Schwartz, T. Smirnova, T. Smith, and G. Manikin, 2004a: An hourly assimilation/forecast cycle: The ruc. *Mon. Wea. Rev.*, **132**, 495–518.
- [6] Benjamin, S. G. G., J. Brown, T. Smirnova, and R. Bleck, 2004b: Mesoscale weather prediction with the ruc20 hybrid isentropic-terrain-following coordinate model. *Mon. Wea. Rev.*, **132**, 473–494.
- [7] Blankenship, C. B., J. L. Case, W. L. Crosson, and B. T. Zavodsky, 2018: Correction of forcing-related spatial artifacts in a land surface model by satellite soil moisture data assimilation. *IEEE Geoscience and Remote Sensing Letters*, **15**, 498–502, doi:10.1109/LGRS.2018.2805259.
- [8] Bonan, G. B., 1996: A land surface model (lsm version 1.0) for ecological, hydrological, and atmospheric studies: Technical description and user's guide. Technical Report 2, NCAR, nCAR/TN-417+STR. URL <http://dx.doi.org/10.5065/D6DF6P5X>
- [9] Bonan, G. B. K. W. O., M. Vertenstein, S. Levis, X. Zeng, Y. Dai, R. E. Dickinson, and Z. Yang, 2002: The land surface climatology of the community land model coupled to the ncar community climate model. *J. Climate*, **15**, 3123–3149.
- [10] Chen, F. and J. Dudhia, 2001: Coupling an advanced land surface-hydrology model with the penn state-ncar mm5 modeling system. part i: Model implementation and sensitivity. *Monthly Weather Review*, **129**, 569–585.
- [11] Chen, F., K. Mitchell, J. Schaake, Y. Xue, H. Pan, V. Koren, Q. Duan, M. Ek, and A. Betts, 1996: Modeling of land-surface evaporation by four schemes and comparison with fife observations. *J. Geophys. Res.*, **101**, 7251, 7268.

- [12] Clapp, R. and G. Hornberger, 1978: Empirical equations for some soil hydraulic properties. *Water Resour. Res.*, **14**, 601, 604.
- [13] Cohen, J. and D. Rind, 1991: The effect of snow cover on the climate. *Journal of Climate*, **4**, 689–706.
- [14] Dai, Y., X. Zeng, R. Dickinson, I. Baker, G. Bonan, M. Bosilovich, A. Denning, P. Dirmeyer, P. Houser, G. Niu,
- [15] K. Oleson, C. Schlosser, and Z. Yang, 2003: Common land model: Technical documentation and user's guide. *Bull. Amer. Meteor. Soc.*, **84**, 1013–1023.
- [16] Deardorff, J., 1978: Efficient prediction of ground surface temperature and moisture with inclusion of a layer of vegetation. *Journal of Geophysical Research*, **83**, 1889–1903.
- [17] Desborough, C. E. A. J. P. and B. McAvaney., 2001: Surface energy balance complexity in gcm land surface models. part ii: coupled simulations. *Climate Dynamics*, **17**, 615–626, doi:10.1007/s003820000131. URL <https://doi.org/10.1007/s003820000131>
- [18] Dickinson, R., A. Henderson-Sellers, P. Kennedy, and M. Wilson, 1986: Biosphere-atmosphere transfer scheme (bats) for the near community climate model. near technical note tn-275 + str.
- [19] Dickinson, R., P. Sellers, and D. Kimes, 1987: Albedos of homogeneous semi-infinite canopies: comparison of two stream analytic numerical solutions. *Journal of Geophysical Research*, **92**, 4282–4286.
- [20] Dudhia, J., 1989: Numerical study of convection observed during the winter monsoon experiment using a mesoscale two-dimensional model.
- [21] Ek, M., K. Mitchell, Y. Lin, E. Rogers, P. Grunmann, V. Koren, G. Gayno, and J. Tarpley, 2003: Implementation of nosh land surface model advances in the national centers for environmental prediction operational mesoscale eta model. *Journal of Geophysical Research*, **108**, 8851.
- [22] Farquhar, G., S. Caemmerer, and J. Berry, 1980: A biochemical model of photosynthetic  $\text{CO}_2$  assimilation in leaves of  $\text{C}_3$  species. *Planta*, **149**, 78–90.
- [23] Feddema, J., K. Oleson, G. Bonan, L. O. Mearns, W. Washington, G. Meehl, and Buja L E, 2005b: The importance of land-cover change in simulating future climates. *Climate Dyn.*, **310**, 1674–1678.
- [24] Feddema, J., K. Oleson, G. Bonan, L. O. Mearns, W. Washington, G. Meehl, and D. Nychka, 2005a: Comparison of a gcm response to historical anthropogenic land cover

- change and model sensitivity to uncertainty in present-day land cover representations. *Climate Dyn.*, **25**, 581–609.
- [25] Garratt, J., 1993: Sensitivity of climate simulations to land-surface and atmospheric boundary-layer treatments - a review. *Journal of Climate*, **6**, 419–449.
- [26] Gilliam, R., C. Hogrefe, and S. Rao, 2006: New methods for evaluating meteorological models used in air quality applications. *Atmospheric Environment*, **40**, 5073–5086, doi:10.1016/j.atmosenv.2006.01.023.
- [27] Gilliam, R. and J. Pleim, 2009: Performance assessment of new land surface and planetary boundary layer physics in the wrf-arw. *Journal of Applied Meteorology and Climatology*, **49**, 760–774.
- [28] Grell, G. and D. Devenyi, 2002: A generalized approach to parameterizing convection combining ensemble and data assimilation techniques. *Geophys. Res. Lett.*, **29**, 38.
- [29] Hong, S., V. Lakshmi, E. Small, F. Chen, M. Tewari, and K. Manning, 2009: Effects of vegetation and soil moisture on the simulated land surface processes from the coupled wrf/noah model. *Journal of Geophysical research*, **114**, doi:10.1029/2008JD011249.
- [30] Jacquemin, B. and J. Noilhan, 1990: Sensitivity study and validation volume 40 of a land surface parameterization using the hapex-mobilhy data set. *Boundary Layer Meteorol.*, **52**, 93–134.
- [31] Koster, R. and M. Suarez, 1992: Modeling the land surface boundary in climate models as a composite of independent vegetation stands. *J. Geophys. Res.*, **97**, 2697–2715.
- [32] Lawrence, D., P. Thornton, K. Oleson, and G. Bonan, 2007: The partitioning of evapotranspiration into transpiration, soil evaporation, and canopy evaporation in a gcm: Impacts on land-atmosphere interaction. *J. Hydrometeorol.*, **8**, 862–880.
- [33] Lawrence, D., X. Zeng, Z. L. Yang, S. Levis, K. Sakaguchi, Bonan, G. B., and G. Andrew, 2011: Parameterization improvements and functional and structural.
- [34] Lokupitiya, R., D. Zupanski, A. Denning, S. Kawa, K. Gurney, and M. Zupanski, 2008: Estimation of global co<sub>2</sub> fluxes at regional scale using the maximum likelihood ensemble filter. *Jour. Geophys. Res.*, **113**, doi:doi: 10.1029/2007JD009679.
- [35] Mahrt, L. and M. Ek, 1984: The influence of atmospheric stability on potential evaporation. *J. Clim. Appl. Meteorol.*, **23**, 222, 234.
- [36] Mahrt, L. and H. Pan, 1984: A two-layer model of soil hydrology. *Boundary Layer Meteorol.*, **29**, 1.
- [37] Manabe, S., 1969: Climate and the ocean circulation: 1, the atmospheric circulation and the hydrology of the earth's surface. *Monthly Weather Review*, **97**, 739–805.



- [38] Miller, N. and Coauthors, 2009: An analysis of simulated california climate using multiple dynamical and statisti- cal techniques. *California Climate Change*.
- [39] Narisma, G. T. and A. J. Pitman, 2006: Exploring the sensitivity of the australian climate to regional land-cover change scenarios under increasing co2 concentrations and warmer.
- [40] Niu, G., Z. Yang, R. Dickinson, and G. E. L., 2005: A simple topmodelâbased runoff parameterization (simtop) for use in global climate models. *J. Geophys. Res.*, **110**, doi:doi: 10.1029/2005JD006111.
- [41] Niu, G. and Y. Z.L., 2004: The effects of canopy processes on snow surface energy and mass balances. *J. Geophys. Res.*, **109**, doi:doi: 10.1029/2004JD004884.
- [42] Niu, G. and Y. Z.L., 2007: An observationâbased formulation of snow cover fraction and its evaluation over large north american river basins. *Geophys. Res.*, **112**, 937–952, doi:doi: 10.1029/2007JD008674.
- [43] Niu, G., Y. Z.L., K. Mitchell, F. Chen, M. Ek, M. Barlage, A. Kumar, K. Manning, D. Niyogi, E. Rosero, M. Tewari, and Y. Xia, 2001a: The community noah land surface model with multiparameterization options (noah - mp). 1: Model description and evaluation with local-scale measurements. *Journal of geophysical research*, **116**, 12109, doi:10.1029/2010JD015139, 2011.
- [44] Niu, G., Y. Z.L., K. Mitchell, F. Chen, M. Ek, M. Barlage, A. Kumar, K. Manning, D. Niyogi, E. Rosero,
- [45] Noilhan, J. and S. Planton, 1989: A simple parameterization of land surface processes for meteorological models. *Monthly weaterh Rev.*, **117**, 536–549.
- [46] Oleson, K. and Coauthors, 2004: Technical description of the community land model (clm). national center for atmospheric research, ncar/tn 4611str.
- [47] Oleson, K. and Coauthors, 2008: Improvements to the community land model and their impact on the hydrological cycle. *Journal of Geophysical Research-Biogeosciences*, **113**.
- [48] Oleson, K., D. Lawrence, and M. e. a. Bonan, G.B. ans Flanner, 2010: Technical description of version 4.0 of the community land model (clm). Technical Report 2, NCAR, nCAR/TN-478+STR.
- [49] Pan, H. and L. Mahrt, 1987: Interaction between soil hydrology and boundary layer development, boundary layer. *Meteorol*, **38**, 185, 202.
- [50] Pan, Z., S. Benjamin, J. Brown, and T. Smirnova, 1994: Comparative experiments with maps on different parame- terization schemes for surface moisture flux and boundary-layer processes. *Mon. Wea. Rev.*, **122**, 449–470.

- [51] Pitman, A. J., 2003: The evolution of, and revolution in, land surface schemes designed for climate models. *International Journal of climatology*, **23**, 479–510.
- [52] Pleim, J. and J. Chang, 1992: A non-local closure model for vertical mixing in the convective boundary layer. *Atmos. En.*, **26**, 965–981.
- [53] Pleim, J. and A. Xiu, 1995: Development and testing of a surface flux and planetary boundary layer model for application in mesoscale models. *Journal of Applied Meteorology*, **34**, 16â32.
- [54] Rosen R. D. 1999: *The global energy cycle*. In Global Energy and Water Cycles, Browning K. A., Gurney R. J. (eds). Cambridge University Press: 1–9.
- [55] Rowntree, P. R., 1983: *Sensitivity of GCM to land surface processes*, Proc. Workshop in Intercomparison of Large Scale Models for Extended Range Forecasts, 225-261.
- [56] Sato, N., P. Sellers, D. Randall, E. Schneider, J. Shukla, J. Kinter, Y. Hou, and E. Albertazzi, 1989: Effects of implementing the simple biosphere model in a general circulation model. *Journal of Atmospheric Sciences*, **46**, 2757–2782, doi:10.1175/1520-0469(1989)046.2757:EOITSB.2.0.CO;2.
- [57] Schaake, J., V. Koren, Q.-Y. Duan, K. Mitchell, and F. Chen, 1996: Simple water balance model for estimating runoff at different spatial and temporal scales. *J. Geophys. Res*, **101**, 7461–7475, doi:10.1029/95JD02892.
- [58] Schaefer, K., P. Tans, S. Denning, I. Baker, J. Berry, L. Prihodko, N. Suits, and A. Philpott, 2008: The combined simple biosphere/carnegie-ames-stanford approach (sibcasa) model, *jour. Geophys. Res*, **113**, doi:doi: 10.1029/2007JG000603.
- [59] Sellers, P., 1985: Canopy reflectance, photosynthesis and transpiration. *Int. J. Remote Sens*, **6**, 1335–1372, doi:doi: 10.1080/01431168508948283.
- [60] Sellers, P., 1992: *Biophysical models of land surface processes. Climate System Modelling*. Cambridge University Press.
- [61] Sellers, P., R. Dickinson, D. Randall, A. Betts, F. Hall, J. Berry, G. Collatz, A. Denning, H. Mooney, C. Nobre,
- [62] Sato, N., C. Field, and A. Henderson-Sellers, 1997: Modelling the exchanges of energy, water and carbon between continents and the atmosphere. *Science*, **275**, 502–509.
- [63] Sellers, P., S. Los, C. Tucker, C. Justice, D. Dazlich, G. Collatz, and D. Randall, 1996a: A revised land surface parameterization (sib2) for atmospheric gcms. part 2: The generation of global fields of terrestrial biophysical parameters from satellite data. *Jour. Clim*, **9**, 706–737.

- [64] Sellers, P., Y. Mintz, Y. Sud, and A. Dalcher, 1986: A simple biosphere model (sib) for use within general circulation models. *Journal of the Atmospheric Sciences*, **43**, 505–531.
- [65] Sellers, P., D. Randall, G. Collatz, J. Berry, C. Field, D. Dazlich, C. Zhang, G. Collelo, and L. Bounoua, 1996b: A revised land surface parameterization (sib2) for atmospheric gcms, part 1: Model formulation. *Jour. Clim*, **9**, 676–705.
- [66] Sellers, P., C. Tucker, G. Collatz, S. Los, C. Justice, D. Dazlich, and D. Randall, 1994: A global  $1^{\circ} \times 1^{\circ}$  ndvi data set for climate studies. part 2: the generation of global fields of terrestrial biophysical parameters from the ndvi. *International Journal of Remote Sensing*, **15**, 3519–3545.
- [67] Skamarock, W., J. Klemp, J. Dudhia, D. Gill, D. Barker, M. Duda, X. Huang, and W. Wang, 2008: A description of the advanced research wrf version 3. near tech. note ncar/tn-4751str.
- [68] Smirnova, T., J. Brown, and S. Benjamin, 1997: Performance of different soil model configurations in simulating ground surface temperature and surface fluxes. *Mon. Wea. Rev.*, **125**, 1870–1884, doi:10.1175/1520-0493(1997)125,1870.
- [69] Smirnova, T., J. Brown, S. Benjamin, and J. Kenyon, 2016: Modifications to the rapid upyear cycle land surface model (ruc lsm) available in the weather research and forecasting (wrf) model. *Monthly weather Review*, **144**, doi:10.1175/MWR-D-15-0198.1.
- [70] Smirnova, T., J. Brown, S. Benjamin, and D. Kim, 2000: Parameterization of cold-season processes in the maps land-surface scheme. *J. Geophys. Res.*, **105**, 4077–4086, doi:10.1029/1999JD901047.
- [71] Smith, T., S. Benjamin, J. Brown, S. Weygandt, T. Smirnova, and B. Schwartz, 2008: *Convection forecasts from the hourly upyeard, 3-km High Resolution Rapid Refresh (HRRR) Model. Preprints, 24th Conf. on Severe Local Storms*. Amer. Meteor. Soc, Savannah, GA.
- [72] Stockli, R., T. Rutishauser, D. Dragoni, P. Thornton, L. Lu, and A. Denning, 2008: Remote sensing data assimilation for a prognostic phenology model. *Jour. Geophys. Res.*, **113**, doi:doi: 10.1029/2008JG000781.
- [73] Subin, Z., W. Riley, J. Jin, D. Christianson, M. Toirn, and L. Kueppers, 2011: Ecosystem feedbacks to climate change in california: Development, testing, and analysis using a coupled reigonal atmosphere and land surface model (wrf3-clm 3.5). *Earth interactions*, **15**, 1–37.

- [74] Tewari, M. and Y. Xia, 2001b: The community Noah land surface model with multiparameterization options (Noah-MP). 2: Evaluation over global river basins. *Journal of geophysical research*, **116**, doi:10.1029/2010JD015140.
- [75] Thompson, G., R. Rasmussen, and K. Manning, 2004: Explicit forecasts of winter precipitation using an improved bulk microphysics scheme. part i: description and sensitivity analysis. *Mon. Wea. Rev.*, **132**, 519–542.
- [76] Verstraete, M. and R. Dickinson, 1986: Modeling surface processes in atmospheric general circulation models. *Annales Geophysicae*, **4**, 357–364.
- [77] Xiu, A. and J. Pleim, 2001: Development of a land surface model. part i: Application in a mesoscale meteorological model. *Journal of Applied Meteorology*, **40**, 192-209.
- [78] Xue, Y., P. J. Sellers, J. L. Kinter, and J. Shukla, 1991: A simplified biosphere model for global climate studies. *Journal of Climate*, **4**, 345–364, doi: 10.1175/1520-0442(1991)004.0345:ASBMFG2.0.CO;2.
- [79] Zheng, D., R. Van der Velde, Z. Su, J. Wen, X. Wang, M. J. Booij, A. Y. Hoekstra, L. Shihua, Y. Zhang, and M. B. Ek, 2016: Impacts of noah model physics on catchment-scale runoff simulations. *Journal of Geophysical Research: Atmospheres*, **121**, 807–832, doi:10.1002/2015JD023695. URL <https://agupubs.onlinelibrary.wiley.com/doi/abs/10.1002/2015JD023695>.

